Synthesis D. Antermite, J. A. Bull Review

Transition Metal-Catalyzed Directed C(sp^3)–H Functionalization of Saturated Heterocycles

Daniele Antermite
James A. Bull*

Department of Chemistry, Imperial College London, White City, Wood Lane, London, W12 0BZ, UK
j.bull@imperial.ac.uk

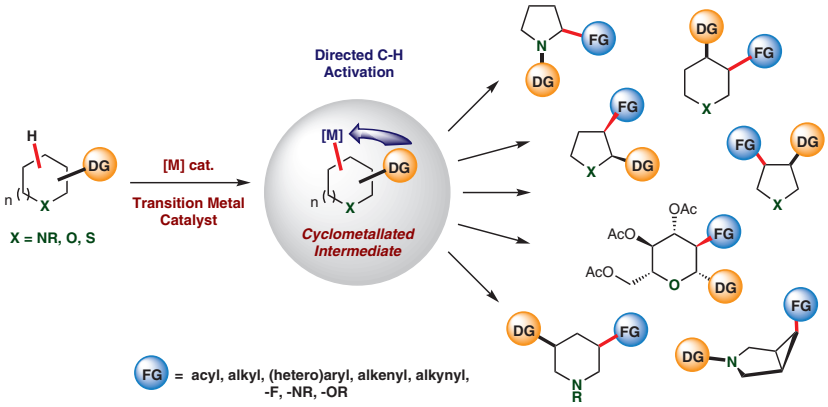

Received: 08.03.2019
Accepted after revision: 03.04.2019
Published online: 17.06.2019
DOI: 10.1055/s-0037-1611822; Art ID: ss-2019-e0164-r

Abstract Synthetic methods that can readily access saturated heterocycles with different substitution patterns and with control of stereo- and regiochemistry are of huge potential value in the development of new medicinal compounds. Directed C–H functionalization of simple and commercially available precursors offers the potential to prepare diverse collections of such valuable compounds that can probe the different available exit vectors from a ring system. Nonetheless, the presence of the Lewis basic heteroatoms makes this a significant challenge. This review covers recent advances in the catalytic C–H functionalization of saturated heterocycles, with a view to different heterocycles (N, O, S), substitution patterns and transformations.

Key words C–H functionalization, saturated heterocycles, transition metal catalysis, stereoselectivity, regioselectivity

1 Introduction

Saturated heterocycles are undoubtedly crucial components in medicinal compounds and natural products.[1,2] Saturated nitrogen and oxygen heterocycles occupy 5 of the top 10 ring structures in drugs.[1a] As such, there is enormous interest in developing efficient, rapid, and divergent synthetic routes to heterocyclic compounds. These present valuable sp^3 rich pharmacophores, fragments for screening, as well as building blocks for the elaboration of core scaffolds.[3,4] As a result, there is considerable demand for methods that can prepare all isomers, to probe the full three-dimensional space around any potential fragment hit or lead compounds, in order to develop biological interactions or selectivity profiles. The ready availability of simple saturated heterocycle derivatives, including enantioenriched derivatives, makes them ideal starting points for further reactions. Therefore, approaches to functionalize existing C–H bonds of these readily available building blocks appear to be of considerable potential.

Over the last 20 years, the concept of transition metal-catalyzed C–H functionalization has emerged with enormous potential to streamline the synthesis of complex molecules.[5] Specifically, transition metal catalysts can activate C–H bonds to form discrete C–M bonds, via different mechanistic pathways.[6] The resulting organometallic intermediate can then form new C–C or C–heteroatom bonds with various coupling partners. Importantly, the use of transition metal catalysts in combination with directing groups enables reactions to occur even at unactivated and less reactive sites. As such, transition metal-catalyzed C–H functionalization is attractive for iterative and divergent synthesis of analogues and for the late-stage functionalization of biologically important compounds.[7] However, in comparison to C–H functionalization at sp^2 carbon centers,[8] C(sp^3)–H functionalization presents problems of lower reactivity and more complex site selectivity and stereochemistry.[9] A popular solution to these problems has been the use of removable directing groups, to position the catalyst appropriately and activate the targeted C–H bond.[10] Seminal works from the groups of Daugulis[11] and Yu[12] on bidentate and monodentate directing groups established the field, and allowed the development of further transformations,[13,14]

more easily removed auxiliaries,[15] and transient directing groups.[16] However, for heterocycles, there are additional concerns that the (protected) heteroatoms would coordinate to the catalyst in competition with the directing group, removing it from the productive cycle.

This review describes transition metal-catalyzed methodologies that have been applied to the direct C(sp^3)–H functionalization of saturated heterocycles from early works up to the end of 2018. The methods included here, all rely on a directing group and proceed via heterocycle–metal bonds.

The review is organized according to the ring position being functionalized and on the type of transformation involved (Scheme 1). This structure is chosen to reflect the products obtained, and the substitution pattern around the heterocycle, rather than the position of functionalization relative to the directing group. The first section of the review covers C–H functionalization at the α-position of the heterocycle, considered to be an activated C–H bond as it is adjacent to the heteroatom. Then C–H functionalization at unactivated positions (i.e., remote from the heteroatom) is additionally classified according to the relative position of the directing auxiliary. Recent examples of transannular C–H functionalization, involving C–H bonds remote from both the heteroatom and the directing group, are described in a separate section.

This review aims to provide the reader with a summary of the reported methods, highlighting significant advances in context of previous works, key mechanistic differences, scope, and limitations. Options for directing group removal, unmasking polar functionalities that can be used as further synthetic handles, are included. Hopefully, this review will constitute a useful tool for synthetic and medicinal chemists for the construction of heterocyclic derivatives, and position these works for future developments in the field.

Other impressive catalytic strategies that can functionalize heterocyclic C–H bonds, particularly at position adjacent to the heteroatom, are outside of the scope of this review. These include metal-catalyzed carbene C–H insertions,[17] photocatalytic oxidative approaches,[18] cross-dehydrogenative couplings,[19] various radical couplings,[20–22] and other innovative processes.[23,24] Importantly, with a few notable exceptions, these strategies do not allow functionalization at C–H positions remote from the heteroatom.[25]

2 α-C–H Functionalization with Directing Group on Nitrogen

The C–H bonds at the α-position adjacent to the heteroatom are relatively weak and this has been extensively exploited to functionalize heterocycles.[26] Traditionally, lithiation and subsequent trapping with electrophiles or transmetalation and catalytic cross-coupling sequences have been used.[27] More recently, selective reaction of the acidic α-C–H has been demonstrated with a variety of transition metal complexes and has been reported most frequently in the presence of an N-linked directing group. This typically consists of a Lewis basic group, containing nitrogen or sulfur, able to coordinate to the metal center to position it in

Biographical Sketches

Daniele Antermite graduated from the University of Bari (Italy), with an M.Sci. degree in Pharmaceutical Chemistry and Technology in 2016. During his undergraduate studies, he performed a training placement in the group of Prof. Stefan Bräse at the Karlsruhe Institute of Technology in Germany. He then carried out his final year project at the University of Vienna (Austria) in the group of Prof. Vittorio Pace, working on lithium halocarbenoids as homologating agents. Daniele is currently a Ph.D. student at Imperial College London (UK) in the Bull group, where he explores new catalytic C(sp^3)–H functionalization strategies to access substituted chiral heterocycles for potential applications in medicinal chemistry.

Dr James Bull is a University Research Fellow at Imperial College London (UK). His research focuses on the development of synthetic and catalytic methods to access medicinally relevant structural motifs and heterocycles. He obtained his M.Sci. degree from the University of Cambridge (UK), then spent a year at GlaxoSmithKline. He returned to University of Cambridge for his Ph.D. with Professor Steven Ley. In 2007 he joined Université de Montréal (Canada) as a postdoctoral researcher with Professor André Charette. He started a Ramsay Memorial Fellowship at Imperial College in 2009, an EPSRC Career Acceleration Fellowship in 2011, and in 2016 was awarded a Royal Society URF.

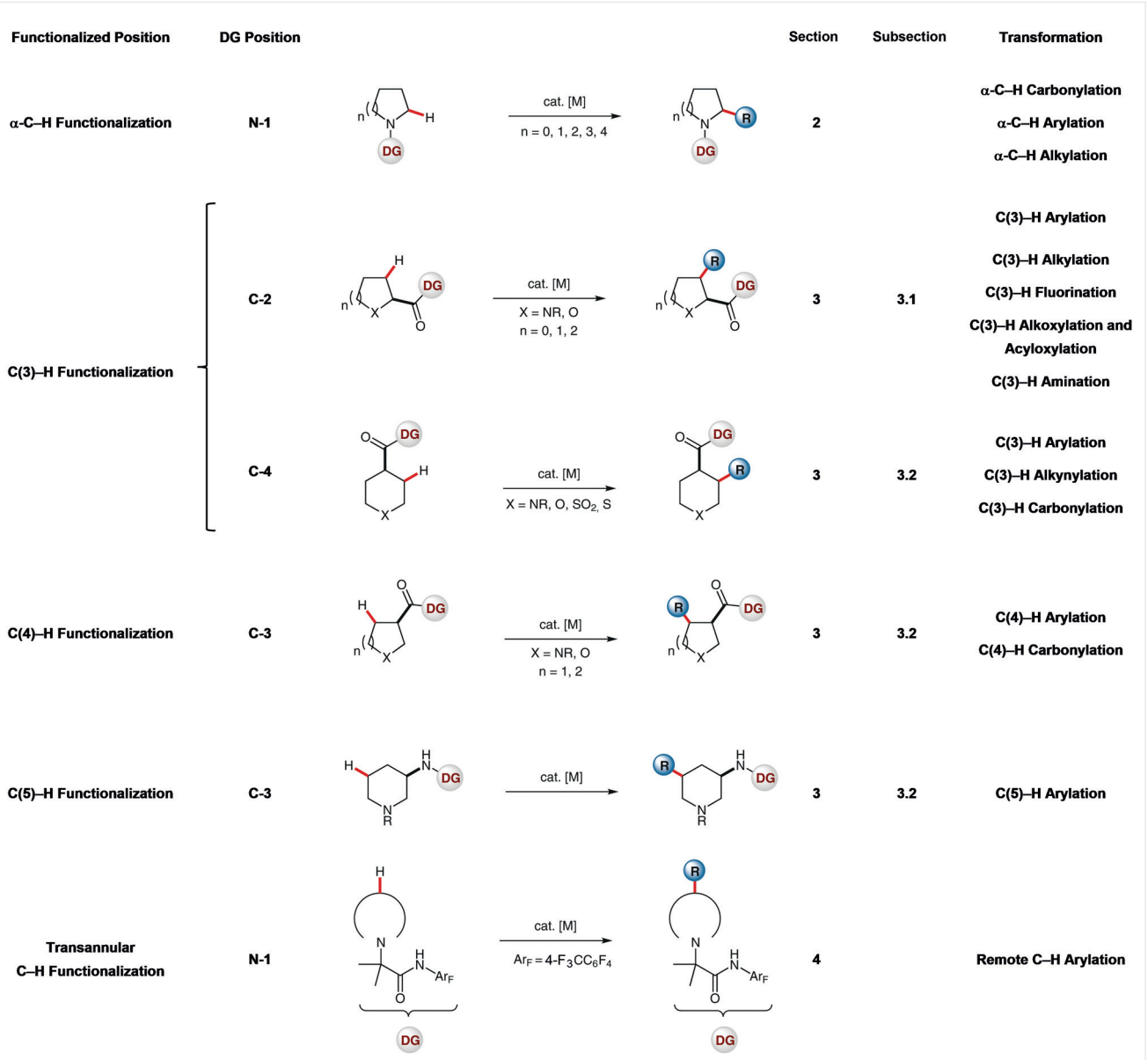

Scheme 1 Summary of transition metal-catalyzed directed C–H functionalization methods on saturated heterocycles

close proximity to the α-C–H bond (Scheme 2). Different coupling partners are then used to intercept the resulting five-membered metallacyclic intermediate, enabling carbonylation, arylation, and alkylation reactions.

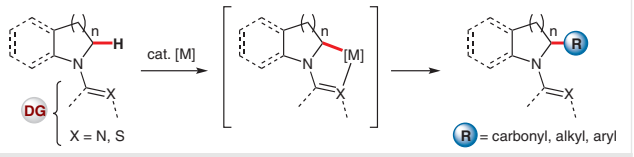

Scheme 2 Directed α-C–H functionalization of saturated nitrogen heterocycles

2.1 α-C–H Carbonylation

The first example of α-C–H functionalization of N-heterocycles via transition metal catalysis was reported by the Murai group in 1997.[28] This seminal report described the Rh-catalyzed carbonylation of *N*-(2-pyridyl)piperazine rings **1** and **2** to give tetrahydropyrazines **4** and **5**, respectively (Table 1). High pressures of CO and ethylene (15 and 10 atm, respectively), as well as high temperature (160 °C), were required to give high conversions. The presence of a pyridine, or pyrimidine, directing group was critical for the success of the reaction, bringing the metal center into close

proximity to the α-C–H bond. Electron-withdrawing substituents on the pyridine ring resulted in higher reactivity, while substituents other than a methyl group at the distal nitrogen gave lower yields.

Table 1 Rh-Catalyzed Carbonylation of *N*-(2-Pyridyl)piperazines and -azepanes[a]

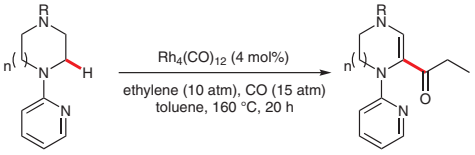

Substrate			Product		Yield (%)
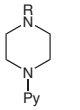	R = Me	**1a**	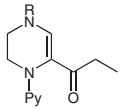	**4a**	85
	CH_2Ph	**1b**		**4b**	44
	4-$MeOC_6H_4$	**1c**		**4c**	37
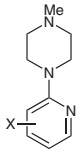	X = 5-CO_2Me	**2a**	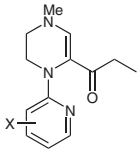	**5a**	93
	5-CF_3	**2b**		**5b**	95
	4-CO_2Me	**2c**		**5c**	83
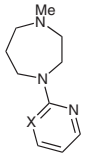	X = CH	**3a**	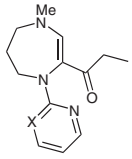	**6a**	65
	N	**3b**		**6b**	84

[a] Py = 2-pyridyl

The corresponding piperidine, morpholine, and piperidin-4-one systems failed to react under otherwise identical conditions, indicating the importance of the 4-nitrogen functionality for the reaction to proceed. This was confirmed by the successful reaction of 1,4-diazepanes **3a** and **3b** which proceeded with excellent regioselectivity. The reaction scope with respect to the olefin was limited to ethylene, while the use of different terminal or cyclic alkenes was unsuccessful. However, when the corresponding tetrahydropyrazine **7** (Scheme 3) was independently treated with CO and hex-1-ene, the carbonylated product was obtained as a mixture of linear and branched isomers. This indicated that ethylene was not only involved as a coupling partner, but also played a crucial role in the initial dehydrogenation of piperazine **1a**. The overall transformation is proposed to proceeded via α-C(sp^3)–H activation and ethylene insertion to form Rh complex **II** (Scheme 3). β-Hydride elimination then gives tetrahydropyrazine **7**, while the active catalytic species is regenerated through reductive elimination of ethane. Finally, α-C(sp^2)–H carbonylation affords the observed product **4a**.

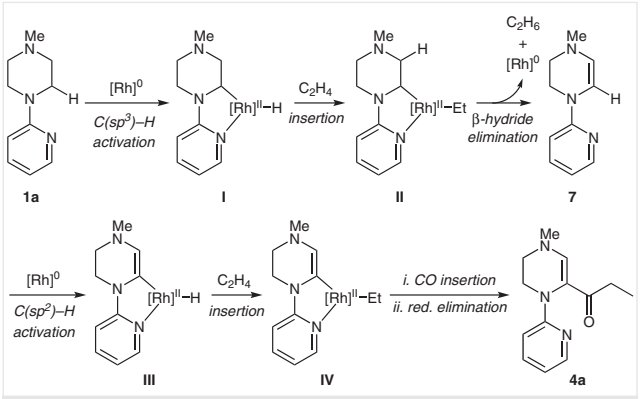

Scheme 3 Proposed mechanism for the Rh-catalyzed carbonylative coupling of piperazines with ethylene

The Murai group also demonstrated that oxygen-based directing groups were able to promote the same reaction of piperazines.[29] In particular, *N*-acetyl and *N*-benzoyl substrates reacted smoothly with CO and ethylene, while only traces of desired product were observed using *N*-Boc as a directing group (Scheme 4).

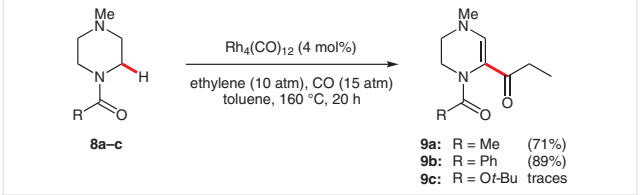

Scheme 4 Carbonylation of *N*-acylpiperazines

A major breakthrough in the field was made in 2000 by the same group, reporting the first example of direct α-C(sp^3)–H carbonylation of *N*-(2-pyridyl)pyrrolidines **10** in the presence of a rhodium catalyst (Table 2).[30] Under these conditions, different heterocycles, including piperidine **11** and tetrahydroisoquinoline **12**, were efficiently functionalized with only traces of dicarbonylation. The efficiency of the reaction was strongly affected by different substituents on the pyridine ring; both electron-withdrawing groups and substituents at the 6-position gave a reduction in yield.

Similar to the mechanism described in Scheme 3, the catalytic cycle starts with coordination of the substrate to the rhodium center. This is followed by activation of the α-C(sp^3)–H bond and ethylene insertion to form an analogous rhodacycle (cf. **II** in Scheme 3). However, in this case, CO insertion is favored over β-hydride elimination and affords saturated products **13–15** after reductive elimination.

Table 2 Rh-Catalyzed C(sp^3)–H Carbonylation of N-Heterocycles[a]

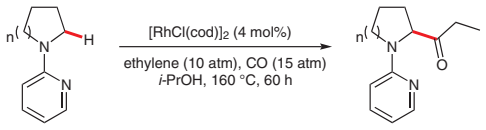

Substrate			Product		Yield (%)
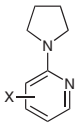	X = H	**10a**	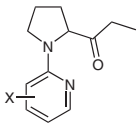	**13a**	68
	3-Me	**10b**		**13b**	73
	5-Me	**10c**		**13c**	84
	6-Me	**10d**		**13d**	12
	5-CF_3	**10e**		**13e**	15
		**11**	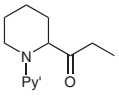	**14**	54
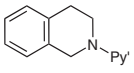		**12**	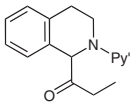	**15**	73

[a] Py′ = 2-[5-(methoxycarbonyl)pyridyl].

2.2 α-C–H Arylation

In 2006, Sames and co-workers first reported the ruthenium-catalyzed C(2)–H arylation of pyrrolidine rings directed by an amidine group (Scheme 5).[31] An excess of ketone (pinacolone) was used to facilitate transmetalation with the arylboronate coupling partner forming intermediate **II**. The Maes group proposed (2010) that transmetalation could also occur directly on Ru^{II}–H complex **I**, suggesting that pinacolone simply acted as a solvent.[32]

In the presence of 3.3 mol% of $Ru_3(CO)_{12}$ and 5 equiv of pinacolone, a variety of electron-rich and electron-poor aryl substituents were installed at the 2-position of *N*-(pyrrolin-2-yl)pyrrolidine and -piperidine rings (Table 3).[31] Heteroarylboronates, including indole and pyridine examples, were also successful under the reaction conditions.

To avoid diarylation, the reaction was performed on 2-functionalized pyrrolidine substrates, forming 2,5-disubstituted products **19** and **20**. Moderate diastereoselectivity was observed in most cases (up to 6:1 dr, *trans*/*cis*). This was found to derive from a fast equilibration of *cis*- and *trans*-isomers under the reaction conditions. Interestingly,

Table 3 Ru-Catalyzed α-Arylation of Pyrrolidines Directed by an *N*-(Pyrrolin-2-yl) Auxiliary[a]

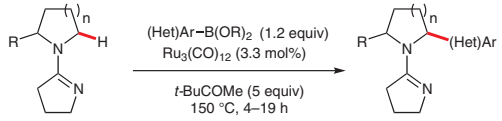

Substrate		Product[b]			Yield (%)	dr[c]
		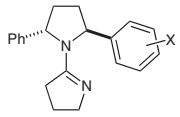	X = H	**19a**	76	3:1
			4-CF_3	**19b**	76	3:1
			4-COMe	**19c**	45	–[e]
			4-OMe	**19d**	70	4:1
			2-Me	**19e**	62	6:1
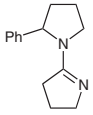	**16**	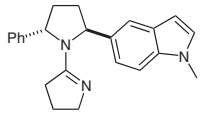		**19f**	62[d]	5:1
		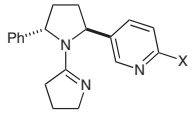	X = H	**19g**	72	3:1
			F	**19h**	63	3:1
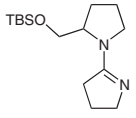	**17**	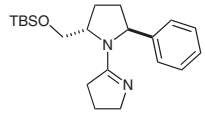		**20**	57	–[e]
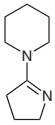	**18**	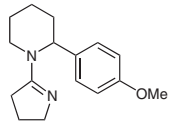		**21**	38	–

[a] Boronic acid pinacol esters or *neo*-pentylglycol esters were used.
[b] Major stereoisomer shown.
[c] Isolated dr.
[d] Using 6.6 mol% $Ru_3(CO)_{12}$.
[e] Single *trans*-product.

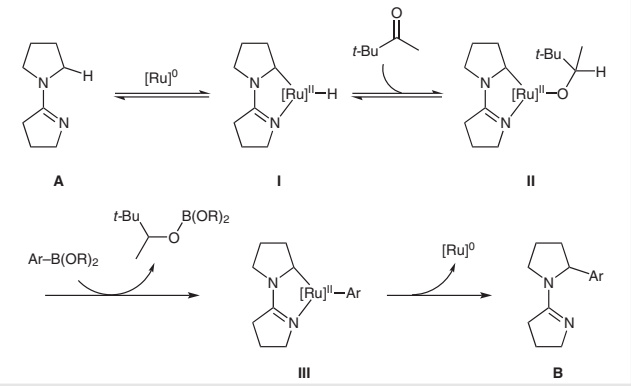

Scheme 5 Proposed mechanism for the Ru-catalyzed α-arylation of *N*-(pyrrolin-2-yl)pyrrolidine with arylboronate esters

in the presence of a methoxycarbonyl group at the 2-position of the ring, insertion of ruthenium catalyst into the acyl C–O bond followed by CO extrusion was favored over α-C–H activation, resulting in a decarboxylative coupling (not shown).[33] Finally, piperidine **18** was less reactive than the corresponding pyrrolidine system, giving monoarylated derivative **21** in 38% yield.

The pyrroline auxiliary was found to be superior to pyridine or pyrimidine in promoting α-arylation, while carbonyl-based *N*-protecting groups were inactive. Importantly, the amidine group could be removed, by treatment with hydrazine and trifluoroacetic acid at 140 °C (Scheme 6).

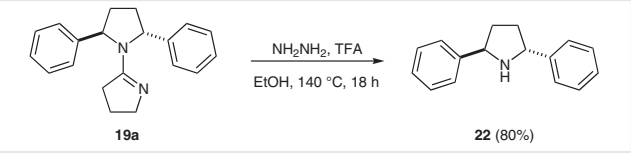

Scheme 6 Pyrroline removal from a 2,5-disubstituted pyrrolidine

Subsequently, the Maes group reported more general conditions for the Ru-catalyzed C(2)–H arylation of *N*-substituted piperidines with (hetero)arylboronate esters.[32] In this case, pyridine was selected as directing group because of its higher stability compared to Sames' pyrroline.[31]

Conditions for pyridine removal were also developed, involving Pd-catalyzed hydrogenation followed by aminolysis with NH_2NH_2/AcOH.[34] Mechanistic investigations suggested a direct transmetalation of Ru^{II}–H complex **II** with boronate esters to be the turnover-limiting step (Scheme 7).

The addition of a tertiary alcohol (*t*-BuOH or 3-ethylpentan-3-ol) was crucial to the success of the catalysis. This was proposed to act as a scavenger for the dialkoxyborane side product **24**, thus avoiding catalyst deactivation. Moreover, best results were obtained when performing the reaction in an 'open vial' under reflux conditions. This set-up was used to release the in situ formed hydrogen gas, which

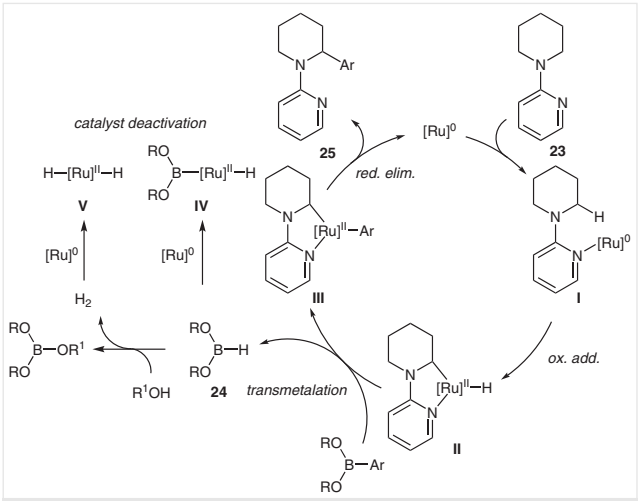

Scheme 7 Proposed mechanism for the Ru-catalyzed α-arylation of *N*-(2-pyridyl)piperidine

could also inhibit the catalyst via oxidative addition. The reaction was tolerant of varied functionalities in the arylboronate coupling partner, including electron-donating and electron-withdrawing substituents at both *para*- and *meta*-positions (Table 4).[32] *Ortho*-Substitution generally resulted in slightly reduced yields.

In most cases mixtures of *cis*- and *trans*-2,6-disubstituted products **26a–g** (in parenthesis, Table 4) were isolated along with the corresponding monoarylated derivatives **25a–g**. However, when using heteroarylboronate esters, no difunctionalization was observed (**25h–j**). The same reaction conditions were also applicable to the α-functionalization of substituted piperidines and related heterocycles such as pyrrolidine **10a**, azepane **29**, and benzannulated derivatives **30a**,**b** (Table 5).[32b] In the presence of C(3) substituents, arylation occurred exclusively at the least hindered α-position, giving 2,5-diarylated piperidines **31a**,**b** with moderate *trans* selectivity. Interestingly, no difunctionalization occurred on azepane **29**, in contrast to the corresponding 5- and six-membered derivatives.

In order to achieve selective monoarylation of piperidine, Schnürch and co-workers proposed the use of a related *N*-[3-(trifluoromethyl)-2-pyridyl] auxiliary under similar reaction conditions (Scheme 8).[35] The CF_3 substituent on the pyridine ring limited the rotational freedom around the C–N bond, thus avoiding the second arylation.

In 2015, the Yu group described in the first palladium-catalyzed α-C–H arylation of saturated N-heterocycles.[36] In the presence of an *N*-thiopivaloyl directing group, pyrrolidine, piperidine, and azepane rings were efficiently coupled with (hetero)arylboronic acids via a Pd^{II}/Pd^0 redox cycle.[37] The use of palladium(II) trifluoroacetate [$Pd(TFA)_2$] as the

Table 4 Ru-Catalyzed α-Arylation of *N*-(2-Pyridyl)piperidine Rings with (Hetero)arylboronate Esters[a]

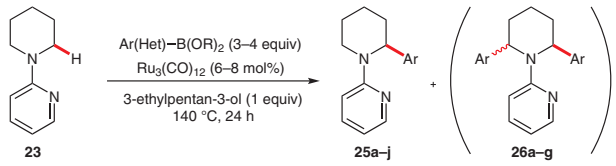

23 25a–j 26a–g

Ar	Product[b]		Yield (%)	dr[c]
	X =			
	H	**25a** (**26a**)	38 (38)	(3:1)
	4-Cl	**25b** (**26b**)	48 (26)	(3:1)
	4-CO_2Me	**25c** (**26c**)	32 (5)	(–[d])
	4-OMe	**25d** (**26d**)	29 (32)	(2:1)
	3-CF_3	**25e** (**26e**)	49 (12)	(3:2)
	3-NH_2	**25f** (**26f**)	36 (30)	(3:1)
	2-Me	**25g** (**26g**)	28 (22)	(5:1)
		**25h**	63	–
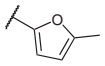		**25i**	65	–
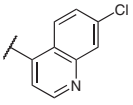		**25j**	50	–

[a] Boronic acid pinacol esters or neo-pentylglycol esters were used.
[b] Monofunctionalized product shown, data for disubstituted product are given in parentheses.
[c] Isolated dr of 2,6-diarylated products (*trans*/*cis*).
[d] Single *trans*-product.

Table 5 α-Arylation of Substituted Piperidines and Related Cyclic Amines[a]

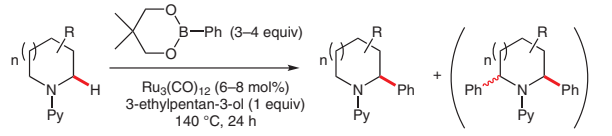

Substrate		Product[b]		Yield (%)	dr
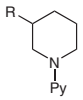	R =		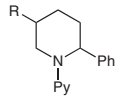		
	3-CF_3	**27a**		**31a**	63	7:3[c]
	3-Ph	**27b**		**31b**	59	4:1[c]
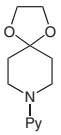		**28**	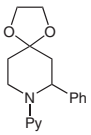	**32** (**33**)	39 (13)	(2:1)[d]
	n =		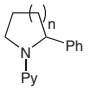		
	1	**10a**		**34a** (**35a**)	25 (36)	(3:1)[d]
	3	**29**		**34b**	54	–
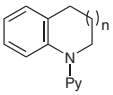	n =		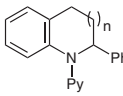		
	1	**30a**		**36a**	91	–
	2	**30b**		**36b**	74	–

[a] Py = 2-pyridyl.
[b] Monofunctionalized product shown, data for disubstituted product are given in parentheses.
[c] Isolated dr of 2,5-disubstituted products (*trans*/*cis*).
[d] Isolated dr of 2,6-disubstituted products (*trans*/*cis*).

catalyst allowed the use of relatively mild conditions for the coupling with a wide array of boronic acids, including heteroaromatic examples (Table 6).[36]

Importantly, no arylation was observed on the *tert*-butyl of the directing group, suggesting a key role of the α-nitrogen in determining site selectivity. In all cases, excellent monoselectivity was achieved (>20:1 mono-/diarylation). This key feature was exploited to successfully develop a one-pot heterodiarylation protocol (Scheme 9).[36] 2,5-Diarylated pyrrolidine **47** was synthesized exclusively as the *trans*-isomer, without requiring a second batch of Pd catalyst.

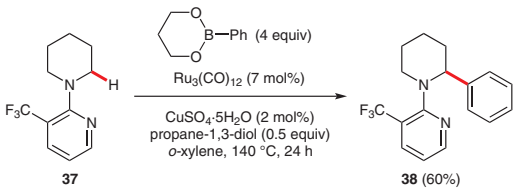

37 38 (60%)

Scheme 8 Selective monoarylation of *N*-[3-(trifluoromethyl)-2-pyridyl]piperidine

In contrast to pyrrolidines, arylation of piperidine ring **42a** was limited by a sluggish reductive elimination (Table 6).[36] To address this issue, a more sterically congested 2,2-diethylbutanethioamide directing group was employed to give product **46b** in high yield.

In this reaction, Pd^{II}-mediated cleavage of the α-C–H bond, through a concerted metalation–deprotonation (CMD),[6b–d] is proposed to produce a palladacycle intermediate **I** (Scheme 10). Transmetalation and reductive elimination affords product **43** with the newly established C–C bond. An excess of 1,4-benzoquinone as external oxidant is essential for catalyst turnover, regenerating the active Pd^{II} species.

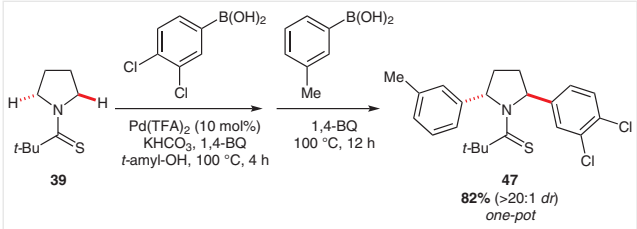

39 47 **82%** (>20:1 *dr*) *one-pot*

Scheme 9 One-pot heterodiarylation of pyrrolidines

Table 6 α-Arylation of Substituted Piperidines and Related Cyclic Amines

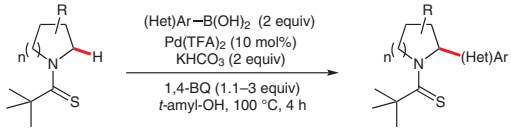

Substrate			Product			Yield (%)
			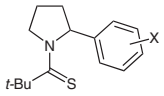	X = 4-COMe	**43a**	80
				4-OCF_3	**43b**	75
				4-NHAc	**43c**	78
				3-Cl	**43d**	79
				2-Me	**43e**	51
		**39**	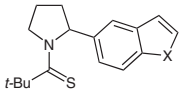	X = O	**43f**	82
				NSO_2Ph	**43g**	77
			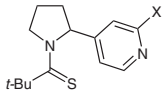	X = F	**43h**	62
				OMe	**43i**	76
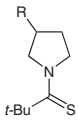	R = 3-Ph	**40a**	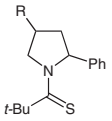		**44a**	74[a]
	3-NHBoc	**40b**			**44b**	87[b]
	3,3-Me_2	**40c**			**44c**	99
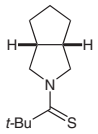		**41**	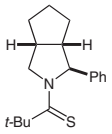		**45**	92[c]
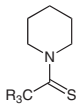	R = Me	**42a**	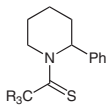		**46a**	13
	Et	**42b**			**46b**	92

[a] 4:1 dr (*trans*/*cis*).
[b] 3:1 dr (*trans*/*cis*).
[c] Single diastereomer (>20:1 dr).

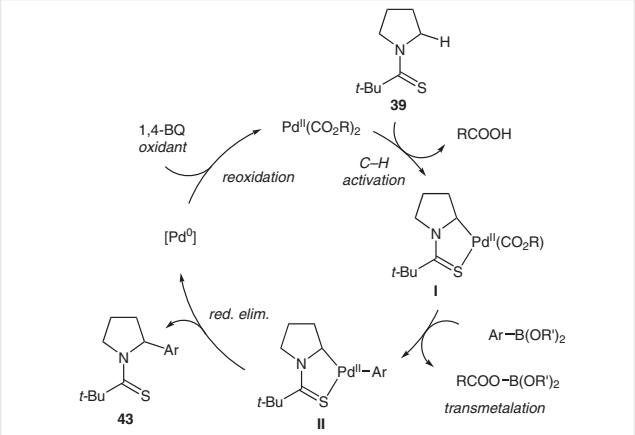

Scheme 10 α-Arylation of saturated aza-heterocycles via Pd^{II}/Pd^0 catalysis

The Yu group also reported a remarkable enantioselective variant of this C(sp^3)–H coupling.[38] This represented the first example of enantioselective C–H arylation of saturated heterocycles, and included four-, five-, six-, and seven-membered rings (Table 7). Differentiation of the enantiotopic α-hydrogens was achieved using a chiral phosphoric acid ligand[39] and a bulky thioamide directing group obtaining high stereocontrol (up to 98% ee). The use of $Pd_2(dba)_3$ as catalyst was important to obtain high enantioselectivity, by minimizing the significant background reaction observed with $Pd(TFA)_2$. This was presumably due to competition of the achiral trifluoroacetate with the chiral phosphate ligand. Notable regioselectivity was observed for indoline **50** and tetrahydroisoquinoline **51**, with no arylation occurring at the *ortho*-C(sp^2)–H and benzylic positions, respectively.[40] However, arylation of tetrahydroquinolines was unsuccessful (<20% yield).

Table 7 Pd-Catalyzed Enantioselective α-Arylation of Saturated Heterocycles

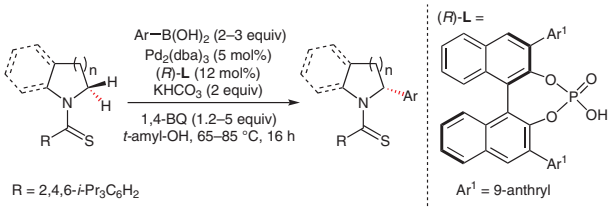

Substrate			Product		Yield (%)	ee (%)
		**48**	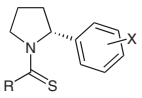	X = 4-OMe **52a** 4-COH **52b** 3-F **52c** 2-Me **52d**	84 71 80 71	97 94 98 94
	n = 0 1 2 3	**49a** **49b** **49c** **49d**	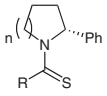	**53a** **53b** **53c** **53d**	40[a] 84[b] 62 54	96 96[b] 91 97
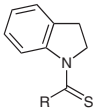		**50**	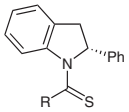	**54**	86	96
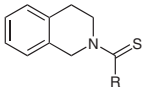		**51**	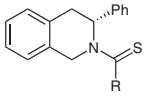	**55**	77	88

[a] 13% diarylated derivative (96% ee, >20:1 dr, *trans*/*cis*).
[b] Gram scale.

Removal of the directing group was accomplishing in two steps with retention of the chiral information (Scheme 11). Reduction with $NiCl_2/NaBH_4$ followed by BCl_3-mediated *N*-debenzylation and Boc protection afforded pyrrolidine **58** in 51% yield and 96% ee over three steps.

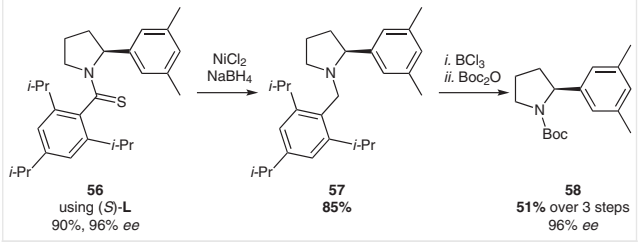

Scheme 11 Removal of thioamide directing group

In 2019, Gong, Zhang, and co-workers described a similar approach for the highly enantioselective α-C–H arylation of *N*-thioamide piperidines and related heterocycles.[41] Excellent asymmetric induction was achieved using an anionic chiral Co(III) complex in combination with a chiral phosphoramidite ligand.

Glorius and co-workers reported the α-C(sp^3)–H coupling of tetrahydroquinolines with aryl iodides under Rh catalysis.[42] High enantioselectivity was obtained using a TADDOL-derived chiral phosphoramidite ligand[43] in combination with 5 mol% of a rhodium(I) precatalyst (Table 8). The *tert*-butylthioamide auxiliary was again employed as optimal directing group. This could be efficiently removed by treatment with NaOMe at 120 °C with no loss of enantiomeric excess. Higher yields and enantioselectivity were generally obtained with more electron-rich iodide coupling partners. Notably, the use of this alternative catalytic system enabled the installation of a boronic acid substituted phenyl group in **62e**, though in lower yield. The same conditions were also applied to the enantioselective monoarylation of other N-heterocycles, for the first time also including a piperazine example **64**. However, a significant reduction in enantioselectivity was observed for pyrrolidine ring **39** (30% ee), displaying the high sensitivity of C–H functionalization reactions to the nature of substrate and catalytic system.

2.3 α-C–H Alkylation

In recent years, significant attention has also been paid to the development of transition metal-catalyzed alkylative couplings of saturated heterocycles. Most of these strategies again involved the use of coordinating N-directing groups, such as pyridine[44,45,47,48,57] or thiocarbonyl[58] moieties, to en-

Table 8 Rh(I)-Catalyzed Enantioselective α-Arylation of Tetrahydroquinolines and N-Heterocycles

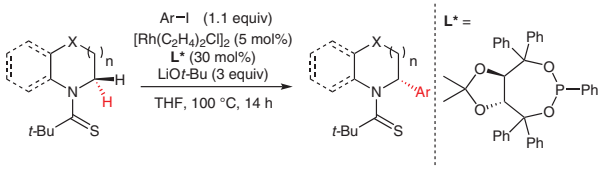

Substrate			Product			Yield (%)	ee (%)
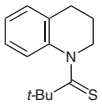		**59**	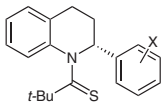	X = H 3-Me 4-*t*-Bu 4-CN 4-Bpin	**62a** **62b** **62c** **62d** **62e**	87 75 83 43 34	91 92 93 71 82
	n = 0 1 2	**60** **39** **42a**	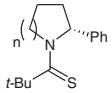		**63a** **63b** **63c**	63 70 80	77 30 85
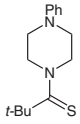		**61**	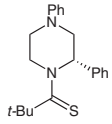		**64**	48	97

able activation of the α-C–H bond. However, a few remarkable examples of α-alkylation of unprotected N-heterocycles have been reported to occur in the absence of any additional directing group.[49–53]

The first example of α-C–H alkylation of azacycles was observed by the Murai group in 2001 during their studies on C(sp^3)–H carbonylative couplings (cf. Table 2).[44] When $Ru_3(CO)_{12}$ was used instead of $[RhCl(cod)]_2$ in the reaction of *N*-(2-pyridyl)pyrrolidine **10a** with ethylene and CO, no carbonylation was observed. Instead, the only product was

Table 9 Ru-Catalyzed α-Alkylation of Saturated N-Heterocycles with Alkenes[a]

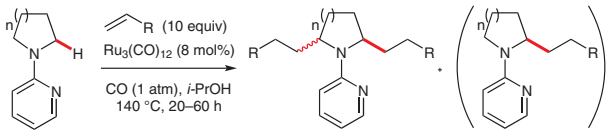

Substrate			Product[b]			Yield (%)	dr[c]
		**10a**	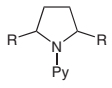	R = Et *n*-Hex $(CH_2)_2$*t*-Bu $(CH_2)_2$Ph Cy	**66a** **66b** (**67b**) **66c** (**67c**) **66d** **66e** (**67e**)	92[d] 53 (29) 73 (21) 58 33 (39)	1:1 1:1 1:1 1:1 1.5:1
	n = 2 3	**23** **29**	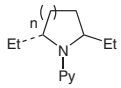		**68a** **68b** (**69b**)	73[d] 14 (47)[d]	1.5:1 1:1
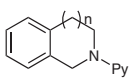	n = 0 1	**65a** **65b**	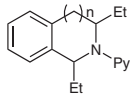		**70a** **70b**	90[d] 85[d]	4:1 3:1

[a] Py = 2-pyridyl.
[b] Disubstituted product shown, data for monosubstituted product are given in parentheses.
[c] Isolated dr of 2,6-disubstituted products (*trans*/*cis*).
[d] Ethylene initial pressure 10 atm.

found to be 2,5-diethylated pyrrolidine **66a**, isolated as a mixture of *cis*- and *trans*-isomers (1:1 dr). These conditions were successfully applied to the coupling of a wide range of saturated heterocycles with terminal and internal alkenes (Table 9).[44] The reaction proceeded with low monoselectivity and dialkylated azacycles **66**, **68**, and **70** were isolated as single or major products. However, monoalkylation was favored when increasing the steric bulk of either the alkene (**67e**) or amine (**69b**) reagents (in parentheses, Table 9).

Although the exact mechanism of the reaction was unclear, the authors suggested the initial formation of a ruthenium–hydride complex **I** via pyridine-directed C(sp^3)–H activation (Scheme 12). Alkene insertion gives intermediate **II**, which undergoes reductive elimination to form alkylated product **B** and regenerate the catalyst. The presence of CO is not necessary for the reaction (which proceeded also under nitrogen atmosphere), but it prevents catalyst deactivation. In order to rationalize the absence of carbonylated product, 2-acylpyrrolidine **13a** was independently synthesized and subjected to standard alkylation conditions (Scheme 13). Interestingly, pyrrolidine **66a** was formed in 81% yield, suggesting a facile decarbonylation reaction occurring in the presence of $Ru_3(CO)_{12}$.

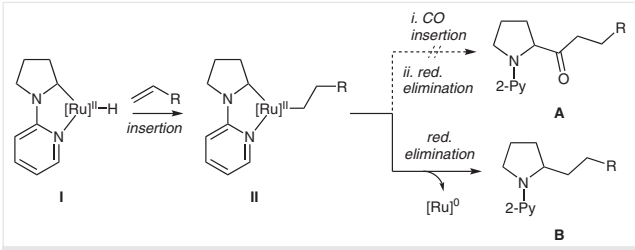

Scheme 12 Proposed mechanism for the Ru-catalyzed α-alkylation of cyclic amines

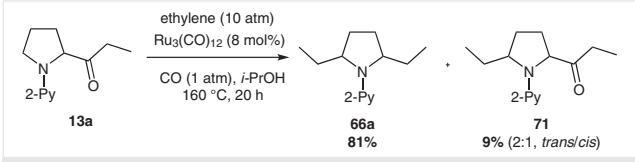

Scheme 13 Decarbonylation under Ru-catalyzed alkylation conditions

Maes and co-workers in 2012 developed alternative conditions for the Ru-catalyzed alkylation of *N*-(2-pyridyl)piperidines.[45] Alkylation of these less reactive substrates was limited by significant hydrogenation of the

Table 10 Ru-Catalyzed α-Alkylation of Substituted Piperidine Rings with Unfunctionalized Alkenes[a]

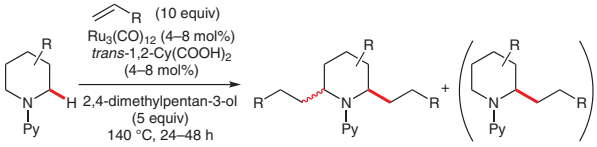

Substrate		Product[b]		Yield (%)	dr
	**23**	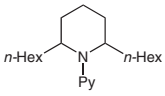	**74** (**75**)	43 (26)	2:1[c]
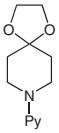	**28**	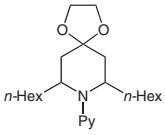	**76** (**77**)	43 (48)	1:1[c]
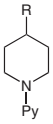	R = OMe CO_2Me Ph	**72a** **72b** **72c**	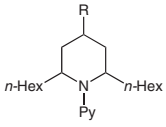	**78a** (**79a**) **78b** (**79b**) **78c**	47 (39)[e] 53 (32)[f] 76	9:3:1[d] 4:1:1[d] 2:6:1[d]
	**73**	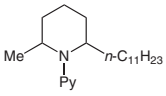	**80**	78	5:3[c]

[a] Py = 2-pyridyl.
[D] Disubstituted product shown, data for monosubstituted product are given in parentheses.
[c] Isolated dr of 2,6-disubstituted products (*trans*/*cis*).
[d] Isolated dr (*cis*,*trans*/*cis*,*cis*/*trans*,*trans*).
[e] 2,4-Disubstituted product (1:1 dr, *trans*/*cis*).
[f] 2,4-Disubstituted product (1:3 dr, *trans*/*cis*).

alkene coupling partner. Moreover, reduction of the ketal moiety was also observed treating piperidine **28** under Murai's original conditions.[44] The combination of a sterically hindered alcohol and a carboxylic acid was crucial to overcome these issues and achieve optimal conversions. In particular, 2,4-dimethylpentan-3-ol and *trans*-cyclohexane-1,2-dicarboxylic acid promoted efficient α-hexylation of piperidines **23**, **28**, **72**, and **73** (Table 10).[45] This protocol also enabled the synthesis of 2-undecylated piperidine **80** in 78% yield, which was readily converted into alkaloid (±)-solenopsin A[46] upon hydrogenative directing group cleavage.[34]

Kinetic studies indicated that the carboxylic acid had a critical effect on the catalytic system. It was found to promote catalyst activation, increase reaction rate, and prevent catalyst deactivation. Moreover, alkylation was favored over hexene reduction as main reaction pathway in the presence of the acidic additive.

However, the acid alone failed to promote the reaction in the absence of a suitable alcohol component. A competitive binding of both alcohol and acid to the metal center is thus proposed. Oxidative addition of the alcohol to Ru^0 forms ruthenium alkoxide **VII** as the only catalytically active species in the absence of acid (Scheme 14). However, β-hydride elimination to give Ru^{II}–H complex **VIII** is favored over alkene insertion and C–H activation requiring a four-membered CMD transition state **X**, resulting in high levels of alkene reduction. This undesired pathway can be slowed down by protonation of the alkoxide by the acid additive (**III**) and formation of Ru–carboxylate **IV**. Alkene insertion and C–H activation, through the more favorable six-membered transition state **XI**, gives metalated piperidine **VI**. Finally, reductive elimination releases alkylated product **75** and regenerates Ru^0.

In 2014, the Maes group extended the scope of this transformation to 3-oxo-functionalized alkenes (Table 11).[47] While the direct use of methyl vinyl ketone was not possible due to its rapid degradation under the reaction conditions, the corresponding dioxolane-protected alkenone was found to be a suitable coupling partner. However, much lower reactivity was observed for this alkene in comparison to unfunctionalized hex-1-ene.[45] Indeed, higher loadings of the alkene (20 equiv) and the alcohol solvent (40 equiv), in combination with catalytic 3,4,5-trifluorobenzoic acid additive, were required to achieve high conversion. Using these optimized conditions, substituted piperidines **27**, **72**, and **73** were alkylated in good to high yields. When using 3-substituted piperidines **27**, exclusive monoalkylation occurred at the least hindered α-position, affording products **83** with preferential *cis*-configuration. A similar stereochemical outcome was obtained with **72** with substituents at C(4), although a small degree of dialkylation was observed in this case. By contrast, for **73** with substituents in the 6-position, the *trans*-isomer became the major product. Interestingly, ethyl 2,2-dimethylbut-3-enoate was

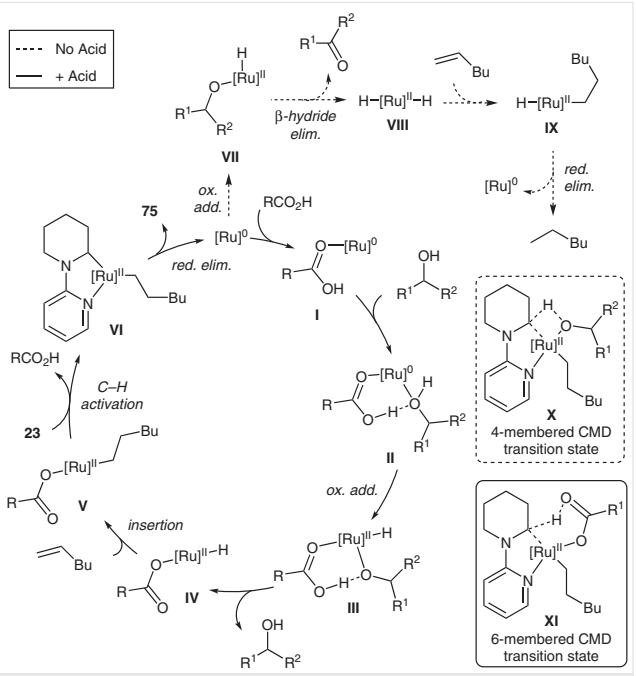

Scheme 14 Proposed catalytic cycle for the Ru-catalyzed alkylation of *N*-(2-pyridyl)piperidines in the presence and absence of a carboxylic acid additive

also effective as the olefin component forming 2,6-disubstituted piperidine **86b** in 87% yield. The efficiency of the alkylation protocol was evaluated on various N-heterocycles, with pyrrolidine **10a** found to be more reactive than the corresponding piperidine system **23**; on the other hand, lower reactivity was observed for azepane **29**. Most notably, the reaction was also successful on *N*-(2-pyridyl) bicyclic amines **81** and **82**, locked in a boat or chair conformation, respectively. Importantly, ketal deprotection was demonstrated on alkylated piperidine **87b**, by treatment with 10 mol% HCl, to unmask the desired ketone functionality (93% yield).

Milder and highly chemoselective conditions for the Ru-catalyzed alkylation of pyrrolidines at C(2) were developed by Ackermann and co-workers.[48] A combination of Ru(II) precatalyst $[RuCl_2(PPh_3)_3]$ and catalytic amounts of BINAP and AgOTf allowed for an efficient reaction even at temperatures as low as 80 °C (Table 12). Notably, varied functionalities in the alkene component, including silanes, enolizable ketones, and alkyl and aryl halides, were well tolerated. An excess of pyrrolidine **10b** was critical to minimize the formation of 2,5-dialkylated products.

Yi and Yun disclosed a ruthenium-catalyzed dehydrogenative coupling of unprotected N-heterocycles with alkenes, occurring in the absence of any directing group.[49] Ruthenium complex $RuHCl(CO)(PCy_3)_2$ was found to sequentially activate both the α-C(sp^3)–H and N–H bonds of cyclic amines, forming 2-substituted cyclic imines **95**, **98**,

Table 11 Ru-Catalyzed α-Alkylation of Substituted Piperidine Rings and Related Cyclic Amines with Functionalized Alkenes[a]

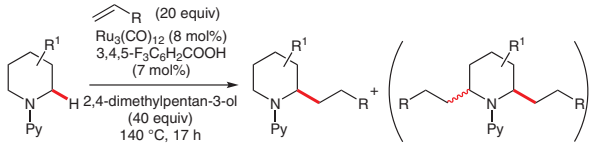

Substrate			R =	Product[b]	Yield (%)	dr
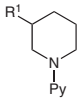	R^1 = CF_3	**27a**		**83a**	63	2:3[c]
	Ph	**27b**		**83b**	75	3:7[c]
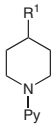	R^1 = CO_2Me	**72b**		**84a** (**85a**)	39 (17)[e]	3:7[d]
	Ph	**72c**		**84b** (**85b**)	34 (18)[f]	3:7[d]
		**73**		**86a**	87	4:1[g]
				**86b**	87	4:1[g]
	n = 1	**10a**		**87a** (**88a**)	46 (38)	4:1[g]
	2	**23**		**87b** (**88b**)	39 (35)	4:1[g]
	3	**29**		**87c** (**88c**)	34 (15)	2:1[g]
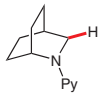		**81**		**89**	47	–
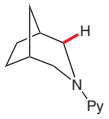		**82**		**90**	30	1:1[h]

[a] Py = 2-pyridyl.
[b] Monosubstituted product shown, data for disubstituted product are given in parentheses.
[c] Isolated dr of 2,5-disubstituted products (*trans*/*cis*).
[d] Isolated dr of 2,4-disubstituted products (*trans*/*cis*).
[e] 2,4,6-Trisubstituted product (8:5:4 dr, *cis*,*trans*/*cis*,*cis*/*trans*,*trans*).
[f] 2,4,6-Trisubstituted product (5:4:9 dr, *cis*,*trans*/*cis*,*cis*/*trans*,*trans*).
[g] Isolated dr of 2,6-disubstituted products (*trans*/*cis*).
[h] Isolated dr (*exo*/*endo*).

and **99** (Table 13). When more sterically demanding 3,3-dimethylbut-1-ene or azepane **94** were used, both imine (**95c** and **99**) and amine (**96** and **100**) products were observed. In contrast, N–H activation products **97** and **101** were formed preferentially in the reaction with vinylsilanes.

Preliminary investigations suggest the formation of a common reactive intermediate **I**, which can undergo either C–H or N–H activation (Scheme 15). The proposed mechanistic pathway involves an amine-directed C(sp^3)–H activation followed by ethylene insertion to give Ru complex **II** (path a). Subsequent β-hydride elimination and C(sp^2)–H alkylation account for the formation of imine derivatives **95**. This is consistent with the formation of ethane detected by NMR. Direct reductive elimination from intermediate **II**, more favorable with bulkier systems, additionally affords alkylated amine **96** (path a′).

On the other hand, when using vinylsilanes the generation of ethylene is observed, and this is proposed to proceed via N–H activation from intermediate **I** followed by β-silyl elimination (path b).

Atom-economical strategies for the α-alkylation of unprotected cyclic amines have been developed involving early transition metal catalysis. Pioneering works from the Hartwig (2007)[50] and the Schafer groups (2009)[51] described the unique ability of tantalum(V) amido **103** and amidate **106** complexes to activate C–H bonds adjacent to nitrogen with no need for protecting/directing groups. Various sec-

Table 12 Ru-Catalyzed Monoselective α-Alkylation of Pyrrolidines

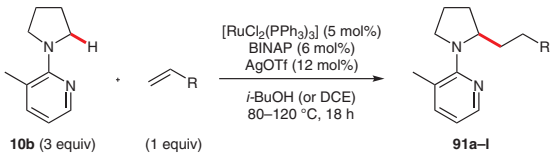

10b (3 equiv) (1 equiv) **91a–l**

Alkene		Product	Yield (%)[a]
	R =		
	n-Bu	**91a**	73
	n-Hex	**91b**	90
	n-$C_{14}H_{29}$	**91c**	87
	t-Bu	**91d**	50
	$SiEt_3$	**91e**	86
	R =		
	Cl	**91f**	82
	Br	**91g**	60
	OTs	**91h**	63
	R =		
	H	**91i**	73
	4-Br	**91j**	65
	2-Br	**91k**	82
		**91l**	40

[a] Yields referred to the alkene coupling partner.

Table 13 Ru-Catalyzed Coupling of Unprotected Cyclic Amines with Alkenes

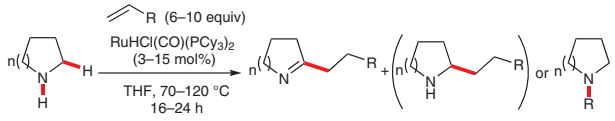

Substrate		Product			Yield (%)[a]
	**92**	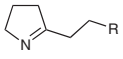	R =		
			H	**95a**	86
			Me	**95b**	51
			t-Bu	**95c** (**96**)	29 (55:45)[b]
			$Si(OEt)_3$	**97**	88
	**93**	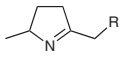	H	**98**	84
	**94**	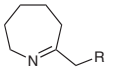	H	**99** (**100**)	87 (60:40)[b]
		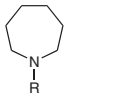	$Si(OEt)_3$	**101**	88

[a] Yields determined by GC.
[b] Imine/amine ratio.

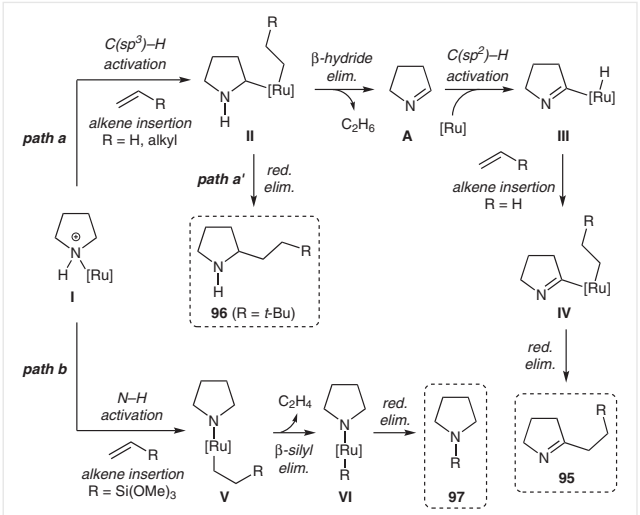

Scheme 15 Proposed mechanism for the Ru-catalyzed C–H and N–H alkylation of unprotected N-heterocycles

ondary amines, including single examples of tetrahydroquinoline **102** and piperidine **105**, were alkylated with terminal, and more recently (2014) internal,[52] olefins in high yields (Scheme 16). In striking contrast with Ru-catalyzed alkylation reactions,[44,45,47,48] branched derivatives **104** and **107** were formed as exclusive products. Chiral amidate complex **108** also enabled alkylation of tetrahydroquinoline **102**, albeit with modest enantioselectivity.[51]

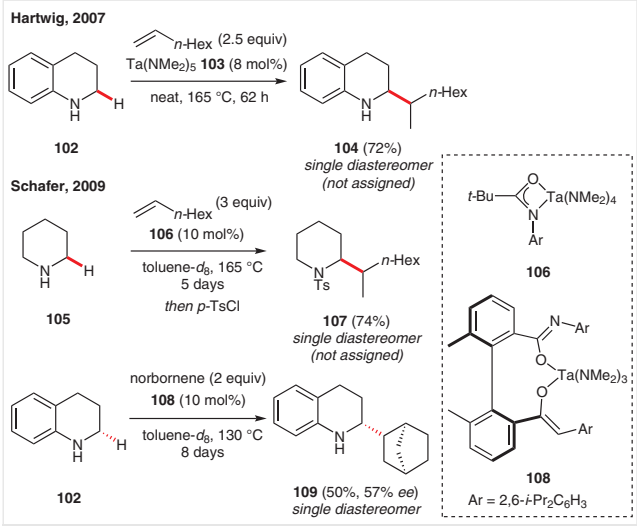

Scheme 16 Early examples of Ta(V)-catalyzed alkylation of unprotected cyclic amines with terminal alkenes

Electrophilic Ta–amidate precatalyst **106** also enabled the direct alkylation of various six- and seven-membered N-heterocycles, including azepane and piperazines derivatives (Table 14).[53]

Table 14 α-Alkylation of Unprotected N-Heterocycles Catalyzed by Ta(V)–amidate Complex

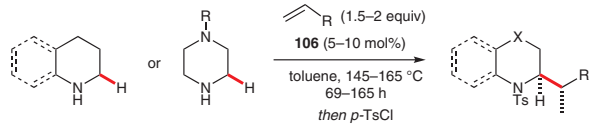

Product		Yield (%)
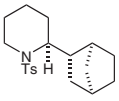	**110**	79
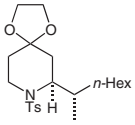	**111**	59
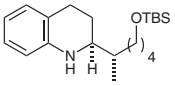	**112**	78[a]
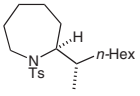	**113**	60
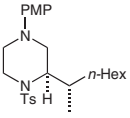	**114**	69
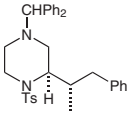	**115**	84

[a] Isolated as the free amine. All products isolated as single diastereomers.

Despite the rather forcing conditions, different functional groups on both amine and alkene reagents were well tolerated, such as silyl ether and acetal groups.

Remarkably, monoalkylated derivatives **110**–**115** were isolated in high yields and excellent diastereoselectivity, usually following N-tosylation. This was likely due to the sensitivity of the catalyst to steric bulk. The proposed mechanism involves initial ligand exchange with the amine substrate, followed by α-C–H activation to form metallaaziridine **I** (Scheme 17). A related three-membered Ta(V) species was previously isolated by the same group and proven to be catalytically competent.[51] Subsequent stereoselective olefin insertion forms five-membered metallacycle **II** in which the pendant alkene substituent is *anti* to the heterocyclic backbone. Finally, proteolysis by the amine reagent and C–H activation regenerates the catalytically active species **I** and liberates the product.

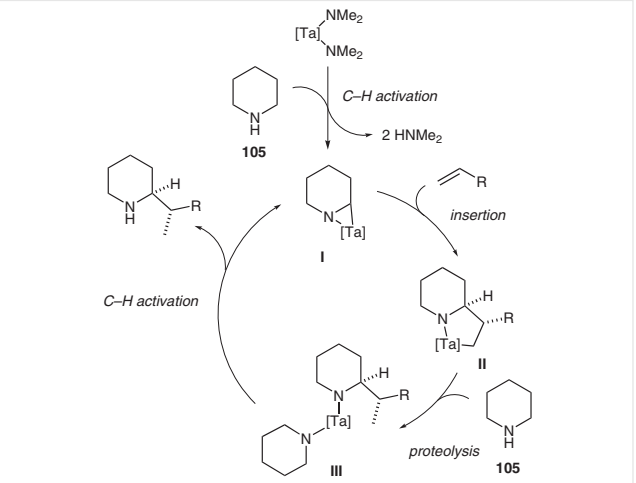

Scheme 17 Proposed mechanism for the Ta(V)-catalyzed alkylation

In 2004, Sames and co-workers first used an iridium(I) complex to catalyze the intramolecular coupling of pyrrolidine α-C–H bonds with alkenes (Table 15).[54] Treatment of *N*-acylpyrrolidine **116** with $[Ir(coe)_2Cl]_2$ and 1,3-bis(2,6-diisopropylphenyl)imidazol-2-ylidene (IPr) carbene ligand gave pyrrolizidinone **117** as the major product, favored over 6-*endo* cyclized indolizidinone **118** (entry 1).

The amount of hydrogenated derivative **119** could be suppressed by addition of norbornene (NBE) or 3,3-dimethylbut-1-ene as hydrogen acceptors (entry 2). On the other hand, using a Rh^0 precatalyst resulted in exclusive intramolecular transfer hydrogenation to give enamine **120** (entry 3).[55] Proline derivative **122** was also successfully cyclized to afford **124** in good yields and with retention of enantiopurity. Interestingly, the reaction did not require a strong N- or S-containing directing group, to enable α-C–H activation. The authors have proposed that π-complex **I**, formed by reaction of the iridium precatalyst with IPr ligand and the substrate, is a key intermediate in the catalytic cycle (Scheme 18); C–H activation of π-complex **I** occurs giving iridium(III) hydride **II**. This complex **II** preferentially undergoes alkene insertion into the alkyl–Ir bond over β-hydride elimination (favored with Rh^0 precatalyst, Table 15, entry 3). The resulting cyclized intermediate **III** then evolves into pyrrolizidinone **117** via β-hydride elimination and alkene isomerization. Finally, hydrogen transfer to norbornene (or substrate) regenerates the active catalytic species. This mechanism is supported by deuteration experiments, as well as by the synthesis and isolation of complex **I**. Importantly, complex **I** was found to be a catalytically competent species in both stoichiometric and catalytic experiments, resulting in almost identical yields and kinetics compared to $[Ir(coe)_2Cl]_2$.

Table 15 Ir-Catalyzed Intramolecular Cross-Coupling of Pyrrolidine α-C–H Bonds with Alkenes

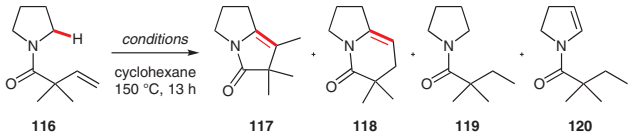

116 117 118 119 120

Entry	Substrate	Conditions[a]	Yield[b] (%)			
			117	**118**	**119**	**120**
1	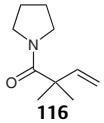 **116**	$[Ir(coe)_2Cl]_2$ (10 mol%), IPr (20 mol%)	41	4	41	–
2		$[Ir(coe)_2Cl]_2$ (10 mol%), IPr (20 mol%), NBE (4 equiv)	66	17	10	–
3		$Cp^*Rh(CH_2CHTMS)$ (5 mol%)	–	–	–	>99
4	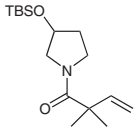 **121**	$[Ir(coe)_2Cl]_2$ (5 mol%), IPr (10 mol%), NBE (3 equiv)	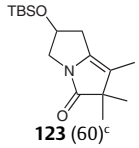 **123** (60)[c]			
5	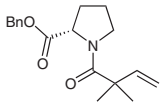 **122** >99% ee	$[Ir(coe)_2Cl]_2$ (5 mol%), IPr (10 mol%), 3,3-dimethylbut-1-ene (10 equiv)	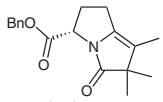 **124** (46)[c] >99% ee			

[a] $[Ir(coe)_2Cl]_2$ = chlorobis(cyclooctene)iridium dimer; NBE = norbornene.
[b] NMR yields.
[c] Isolated yields.

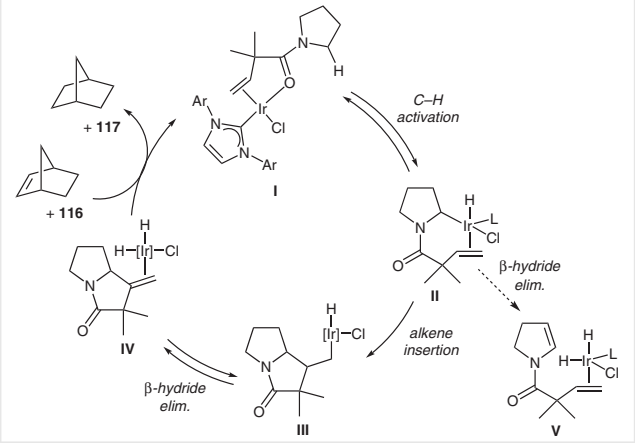

Scheme 18 Proposed catalytic cycle for the Ir-catalyzed intramolecular cyclization of *N*-acylpyrrolidine

In 2014, Opatz and Lahm used a removable benzoxazole auxiliary to direct the Ir-catalyzed intermolecular α-alkylation of saturated azacycles.[56] *N*-(Benzoxazol-2-yl)tetrahydroisoquinoline **125** was coupled with a wide array of activated and unactivated terminal olefins with excellent C(3) regioselectivity (Table 16). Different functionalities, including esters, silanes, and boronic esters, could be successfully installed. Tetrahydroquinolines **126** and piperidine **127** were also effective substrates giving good to excellent yields of monoalkylated products **129** and **130**, respectively. In contrast, the corresponding pyrrolidine derivative resulted in poor yield and selectivity. The benzoxazol-2-yl group could be removed under basic or reductive conditions. As an example, treating alkylated derivative **128c** with $LiAlH_4$ in THF at reflux for two days gave the corresponding unprotected amine in 57% yield.

A chiral cationic Ir^I catalyst was employed by Shibata and co-workers to effect the enantioselective α-C(sp^3)–H alkylation of *N*-(2-pyridyl)pyrrolidin-2-one (γ-butyrolactam) **131** (Table 17).[57] Best results were obtained with Ir–tol-BINAP, which was formed in situ from $[Ir(cod)_2]BF_4$ and chiral phosphine ligand (*S*)-tolBINAP. Various electron-deficient terminal alkenes were successful and 5-alkylated lactams **132** were obtained with good levels of enantioinduction, though requiring very long reaction times. Removal of the pyridine directing group was achieved adapting the hydrogenation/hydride reduction protocol reported by the Maes group.[34] Crucially, the enantiomeric excess was preserved, providing access to enantioenriched γ-amino acid **134** after lactam hydrolysis (Scheme 19).

In 2017, the Yu group extended the use of sulfur-based directing groups to the Ir(I)-catalyzed α-alkylation of pyrrolidine rings.[58] The use of an alternative *N*-alkoxythiocarbonyl auxiliary, readily accessible from pentan-3-ol, proved to be optimal for this transformation. Moreover, simple treatment with TFA at 65 °C allowed for its efficient cleav-

Table 16 Benzoxazole-Directed Intermolecular C(2) Alkylation of Tetrahydroisoquinolines and N-Heterocycles[a]

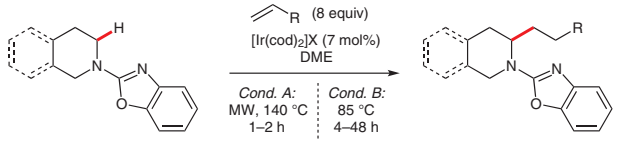

Substrate		Product			Yield (%)
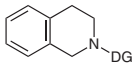	**125**	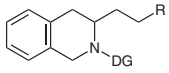	R =		
			n-Bu	**128a**	83
			Bn	**128b**	78
			Ph	**128c**	81
			CO_2Et	**128d**	84
			CO_2Me	**128e**	78
			$SiMe_3$	**128f**	41
			Bpin	**128g**	61
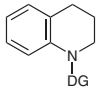	**126**	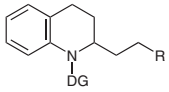	R =		
			CO_2Et	**129a**	95
			Ph	**129b**	73
			$SiMe_3$	**129c**	81
	**127**	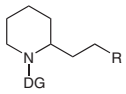	R =		
			CO_2Et	**130a**	57
			Ph	**130b**	48
			$SiMe_3$	**130c**	39

[a] DG = benzoxazol-2-yl directing group; BARF = tetrakis[3,5-bis(trifluoromethyl)phenyl]borate.

Table 17 Enantioselective α-Alkylation of *N*-(2-Pyridyl)pyrrolidin-2-one Catalyzed by a Cationic Ir(I) Complex

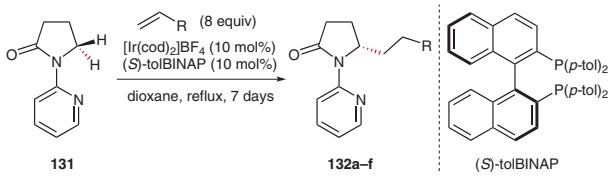

R	Product	Yield (%)	ee (%)
Ph	**132a**	85	82
4-$CF_3C_6H_4$	**132b**	87	85
CO_2Me	**132c**	82	91
CO_2Et	**132d**	87	91
SO_2Ph	**132e**	70	82
P(O)$(OEt)_2$	**132f**	82	76

age. In the presence of $[Ir(cod)_2]OTf$, pyrrolidine **135** reacted smoothly with a large variety of terminal olefins bearing various pendant functionalities (Table 18).

Reducing the alkene loading or the reaction time did not improve the monoselectivity, and 2,5-dialkylated derivatives **139** were generally formed as major or exclusive products. The reaction was sensitive to the steric nature of the substrates, and more hindered pyrrolidines **136** and **137** were monoalkylated in lower, but synthetically useful,

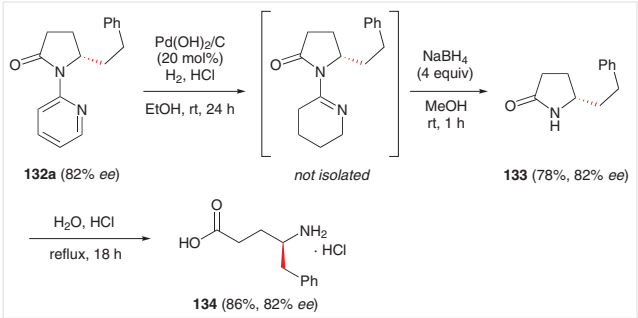

Scheme 19 Synthesis of an enantioenriched γ-amino acid

yields. Notably, biologically relevant L-proline derivative **138** was monoalkylated in good yield and moderate diastereoselectivity.

3 C–H Functionalization at Unactivated C(3), C(4), and C(5) Positions

There are markedly fewer examples of C(sp^3)–H functionalization of saturated heterocycles at positions remote from the heteroatom. This reflects the lower reactivity of these methylene C–H bonds, generally referred to as 'unactivated'. To date, successful strategies have involved the use of palladium catalysis in combination with mono- or bidentate directing groups. In particular, Daugulis' 8-aminoquinoline auxiliary[11] has been used for the C–H functional-

Table 18 Ir(I)-Catalyzed α-Alkylation of Pyrrolidines and Related Azacycles Directed by an Alkoxythiocarbonyl Auxiliary

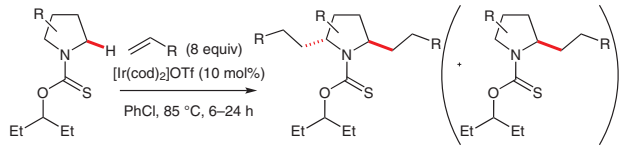

Substrate		Alkene	R	Product[a]	Yield (%)
	**135**		CO_2Et	**139a** (**140a**)[b]	68
			Bu	**139b** (**140b**)[c]	62
			Cy	**139c**	52
			CN	**139d**	40
			SO_2Ph	**139e**	55
			$4\text{-}FC_6H_4$	**139f**	96
		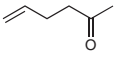		**139g**	73
				**139h**	70
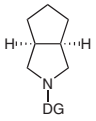	**136**			(**141**)[d]	42
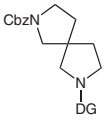	**137**	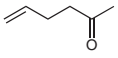		(**142**)[d]	40
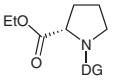	**138**			(**143**)[d]	48[e]

[a] Disubstituted product shown, data for monosubstituted product are given in parentheses.
[b] di/mono = 1.8:1.
[c] di/mono = 1.2:1.
[d] Single monoalkylated product.
[e] 6:1 dr (*trans*/*cis*).

ization of various heterocycles. Regioselective β- or γ-functionalization of carboxylic acid or amine derivatives, respectively, allowed for different substitution patterns to be obtained, depending on the position of the directing group (Scheme 20).

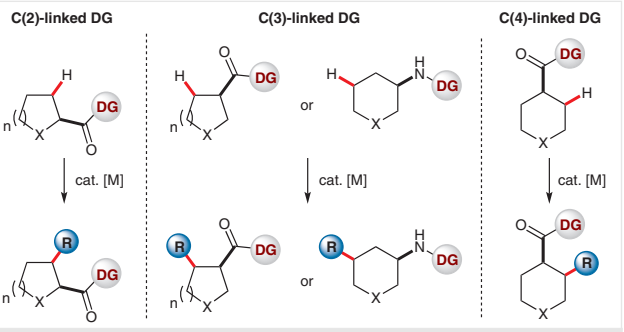

Scheme 20 Directed C(sp^3)–H functionalization of saturated heterocycles at unactivated positions

3.1 C–H Functionalization at C(3) with Directing Groups at C(2)

3.1.1 C(3)–H Arylation

The first example of C–H arylation of L-proline derivatives was developed by Bull and co-workers in 2014, using palladium catalysis and 8-aminoquinoline (AQ) amide at C(2) to direct arylation at the unactivated 3-position.[59] Importantly, the reaction with aryl iodides was highly stereoselective and 2,3-disubstituted derivatives **145** were obtained in high yields as single *cis*-diastereomers (Table 19). The enantiomeric excess of proline was completely retained, providing enantiopure *cis*-arylated products. In comparison to cycloalkyl analogues,[11b,60] the reactivity was reduced, requiring the reaction to be performed under solvent-free conditions. The best results were obtained using 5 mol% $Pd(OAc)_2$ and AgOAc, requiring only 1.8 equiv of aryl iodide. Under the optimized conditions, *N*-Cbz-L-prolin amide **144** was coupled with a wide range of aryl, heteroaryl, and vinyl iodides, containing both electron-donating and -withdrawing groups in good to excellent yields.[59] The choice of *N*-protecting group was of critical importance, with a reactivity drop observed for the *N*-Boc analogues. In this case, a longer reaction time of 72 h and an increased catalyst loading (10 mol%) were required to achieve optimal conversion.[61] Importantly, the same stereochemical outcome was observed, compared to the *N*-Cbz substrate. Liu, Zhang, and co-workers also reported related conditions to successfully effect the C(3)–H arylation of *N*-pivaloylproline derivatives.[62]

The reaction is proposed to proceed through a Pd^{II}/Pd^{IV} redox cycle (Scheme 21).[11b,59,63] Directing group coordination to the metal center is followed by a concerted metalation–deprotonation to form five-membered Pd^{II} metallacycle **II**. Oxidative addition with an aryl iodide then gives Pd^{IV} complex **III**, which undergoes reductive elimination to form the new C–C bond. The *cis*-selectivity results from the requirement for a 5,5-*cis*-fused palladacycle **II**. Preferred C–H activation *cis* to the directing group is supported by deuteration experiments independently performed on the same substrate.[64] Halide abstraction by Ag(I) and proteolysis of complex **IV** liberates the product and regenerates the active Pd^{II} species.

Removal of the aminoquinoline was unsuccessful under many hydrolytic conditions. As an alternative, 5-methoxy-8-aminoquinoline (5-OMe-AQ),[15b] gave similar results to AQ for proline C(3)-arylation (Scheme 22). Oxidative cleavage of this auxiliary with ceric(IV) ammonium nitrate (CAN) occurred readily affording free amides **148** in high yields.[59] Subsequent Cbz deprotection provided access to 3-arylprolinamides **149** of interest as fragments and building blocks in medicinal chemistry.

Table 19 Pd-Catalyzed C(3)-Arylation of Proline Amide **144** with Aryl Iodides

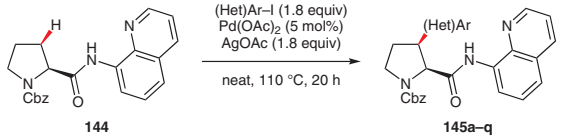

144 **145a–q**

Ar–I		Product	Yield[a] (%)
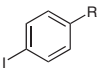	R =		
	Me	**145a**	91
	F	**145b**	88
	Cl	**145c**	78
	Br	**145d**	68
	OMe	**145e**	85
	CO_2Et	**145f**	90
	COMe	**145g**	74
	R =		
	CF_3	**145h**	76
	CN	**145i**	59
	NO_2	**145j**	74
		**145k**	44
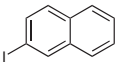		**145l**	73
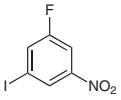		**145m**	70
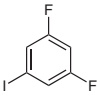		**145n**	60
		**145o**	87
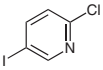		**145p**	54
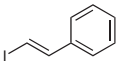		**145q**	51

[a] Products isolated as single enantiomers and *cis*-diastereomers.

In 2016, Maulide and co-workers described an efficient oxidative cleavage of the aminoquinoline directing group by ozonolytic fragmentation and aminolysis or hydrolysis of the resulting intermediate **I**.[65] This was demonstrated on pyrrolidine substrate **145a**, increasing the synthetic utility of the above C–H arylation approach (Scheme 23).

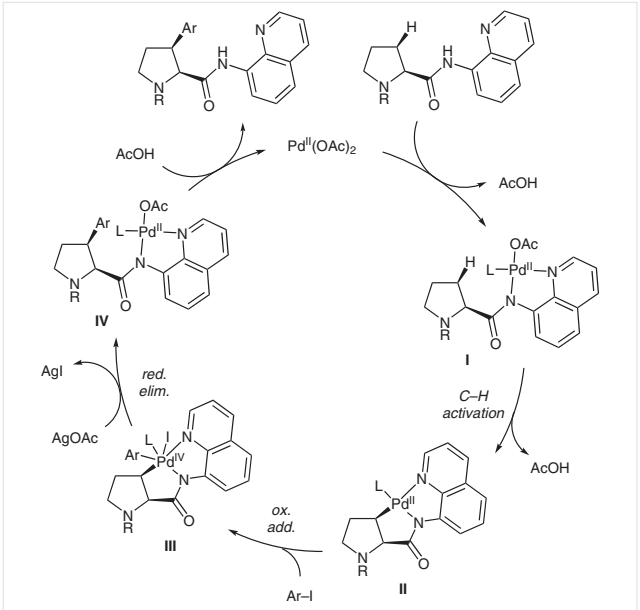

Scheme 21 α-Arylation of proline derivatives by Pd^{II}/Pd^{IV} catalysis

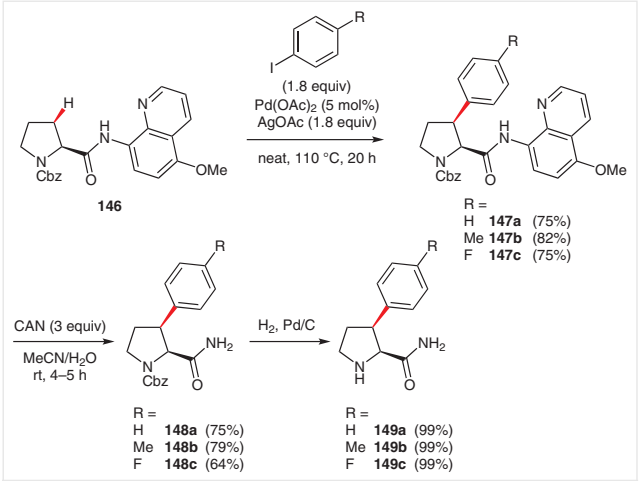

Scheme 22 Synthesis of medicinally relevant primary amides by both directing group removal and Cbz deprotection; products isolated as single enantiomers and *cis*-diastereomers

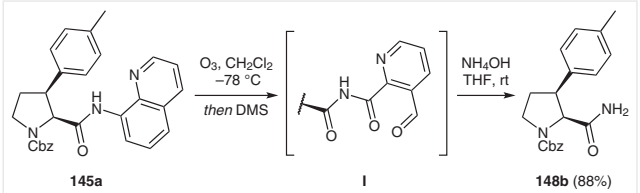

Scheme 23 Ozonolytic cleavage of AQ directing group

The AQ auxiliary has since been shown to be highly effective for the C(3)–H arylation of various related N- and O-heterocycles, including piperidines,[61,66,68] azetidines,[70] γ-lactams,[72] and 5- and six-membered cyclic ethers.[61,73,74]

In 2016, Bull and co-workers extended their C–H arylation protocol to piperidine rings.[61] The six-membered derivatives were much more reactive than the pyrrolidine analogues, presumably due to a reduced strain in the metallacyclic intermediate. Both *N*-Cbz **150** and *N*-Boc **151** substrates were successfully arylated under slightly different conditions, affording exclusively *cis*-configured products **152** and **153** in good to excellent yields (Scheme 24). Bromobenzene was also found to be a competent coupling partner. The excellent *cis*-selectivity was likely derived from a preferential conformation of the ring with the directing group in the axial position to minimize 1,3-allylic strain with the *N*-carbamate group.

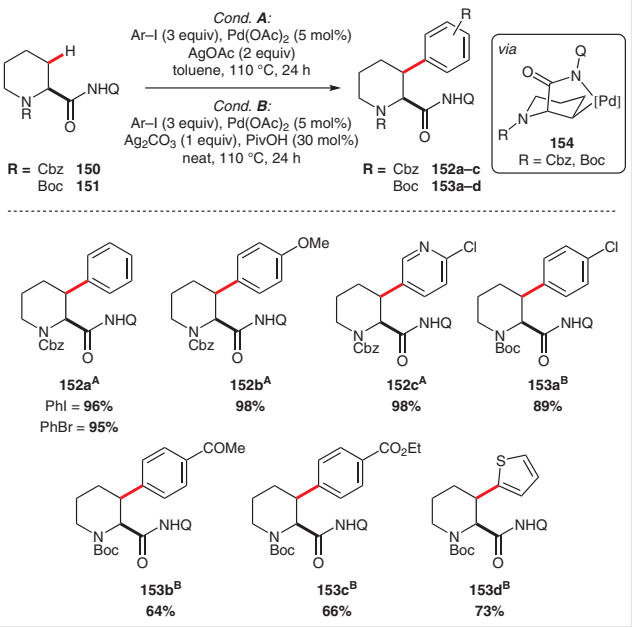

Scheme 24 Pd-catalyzed arylation of *N*-(quinolin-8-yl)piperidine-2-carboxamide derivatives; products isolated as single *cis*-diastereomers; Q = quinolin-8-yl

The same stereochemical outcome was observed by Wu, Cao, and co-workers in 2016–2017 who independently reported similar conditions for the arylation of *N*-Cbz-piperidine at C(3).[66] The superior reactivity of the piperidine system was similarly observed in this study and various aryl groups, including *ortho*-substituted examples, were installed in high yields (up to 96%).[66a] The synthetic utility was highlighted in the stereocontrolled synthesis of (–)-preclamol [(–)-3-PPP, **160**], a dopaminergic autoreceptor agonist.[66b,67] Key C(3)–H arylation of (–)-L-pipecolinic acid derivative **155** was followed by a two-step AQ removal and radical decarboxylation (Scheme 25). Finally, protecting group interconversion and phenol deprotection gave bioactive compound **160**.

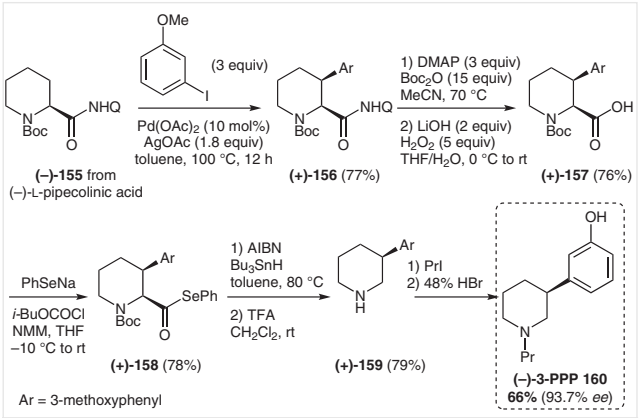

Scheme 25 Synthesis of (–)-preclamol through a stereocontrolled C(sp^3)–H arylation of a piperidine derivative; Q = quinolin-8-yl

At a similar time in 2016, Kazmaier and co-workers extended the scope of AQ-assisted C(3)–H arylation to small di- and tripeptides containing pyrrolidine and piperidine rings.[68] The reaction was optimized on racemic 1-Gly-piperidine-2-carboxamide and then exploited for the arylation of enantiopure substrates **161** with different aryl iodides (Scheme 26). Complete *cis*-diastereoselectivity was again observed in all cases.

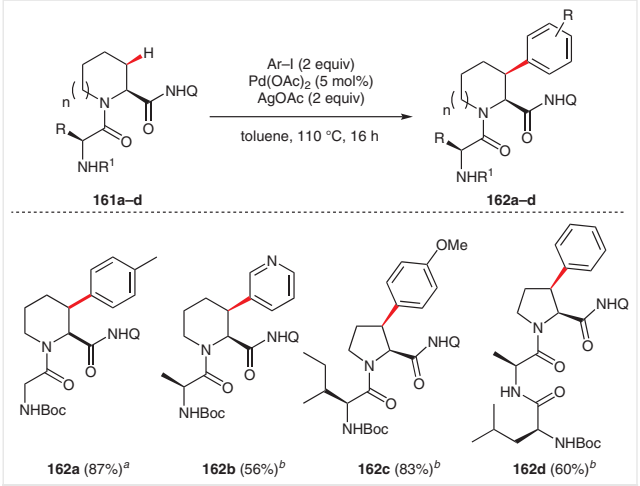

Scheme 26 Pd-catalyzed arylation of piperidine- and pyrrolidine-containing peptides; Q = quinolin-8-yl. [a] Single *cis*-diastereomer. [b] Isolated as single enantiomers and diastereomers.

An alternative strategy for the β-C(sp^3)–H arylation of piperidines at unactivated positions was disclosed by Stamos, Yu, and co-workers involving the use of NHC ligands in combination with palladium(II) trifluoroacetate

[Pd(TFA)$_2$].[69] Ligands bearing bulky tertiary alkyl substituents performed best in the presence of a weakly coordinating amide auxiliary (Table 20).

Table 20 Ligand-Enabled Pd^{II}-Catalyzed C(3)-Arylation of 1-(Trifluoroacetyl)-Substituted Piperidine-2-carboxamides

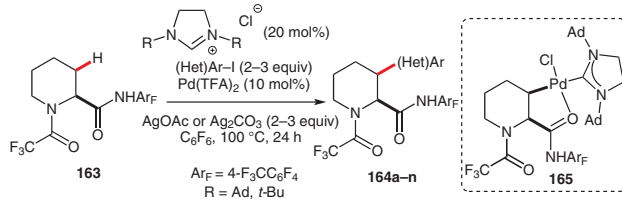

Ar–I		Product[a]	Yield (%)
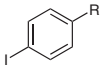	R =		
	Me	**164a**	98
	OTBS	**164b**	90
	CF_3	**164c**	79
	CHO	**164d**	53
	NHBoc	**164e**	94
	$CH_2PO(OEt)_2$	**164f**	73
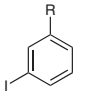	R =		
	CO_2Me	**164g**	93
	CH_2OAc	**164h**	82
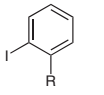	R =		
	OMe	**164i**	83
	NHAc	**164j**	70
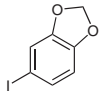		**164k**	88
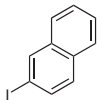		**164l**	91
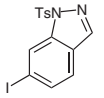		**164m**	48
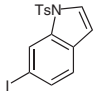		**164n**	60

[a] Products isolated as single *cis*-diastereomers.

1-(Trifluoroacetyl)piperidine-2-carboxamide **163** was arylated with a broad range of aryl and heteroaryl iodides, affording *cis*-2,3-disubstituted derivatives **164** in good to excellent yields. Much lower reactivity was observed for the corresponding pyrrolidine-2-carboxamide, which gave only 28% of C(3)-arylated product. Based on preliminary experimental observations, including isolation of Pd^{II}/NHC complex **165**, a Pd^{II}/Pd^{IV} catalytic cycle is proposed to operate.

The Schreiber group developed the first Pd-catalyzed C(3)–H arylation of azetidine-2-carboxylic acid derivatives, providing a much-improved route to BRD3914, a potent antimalarial compound (Scheme 27a).[70] A series of bioactive bicyclic azetidines was discovered by the same group through a diversity oriented synthesis (DOS) guided investigation into novel antimalarials.[71] The lengthy synthetic route (14 steps to BRD3914) limited the potential to access analogues for systematic evaluation of *in vivo* activity. C–H Functionalization was thus targeted to increase synthetic flexibility through arylation of *N*-(quinolin-8-yl)azetidine-2-carboxamide. Conditions suitable for pyrrolidines and piperidines were not effective. Ultimately, success was obtained using a phosphate ester additive to facilitate the concerted metalation–deprotonation step to form the sterically congested 4-5-5 fused palladacyclic intermediate **169** (Scheme 27b). The *N*-trifluoroacetyl group on the azetidine was important for the arylation reaction and could be advantageously removed as part of the workup. The application of a range of aryl iodides and heteroaryl iodides generated arylated azetidines **168**.

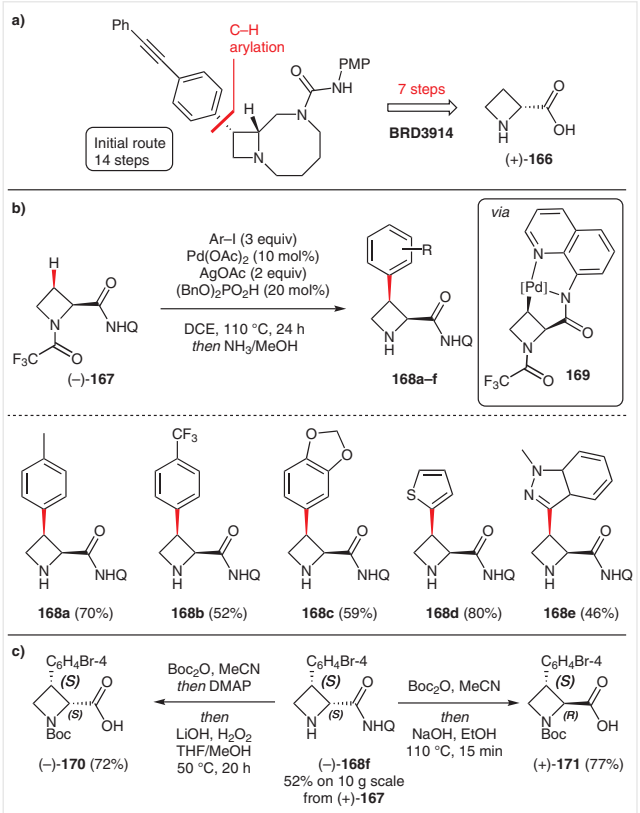

Scheme 27 (a) Route to BRD3914. (b) Pd-catalyzed *cis*-arylation of *N*-(quinolin-8-yl)azetidine-2-carboxamide; products isolated as single enantiomers and diastereomers. (c) Stereocontrolled directing group removal.

The C–H arylation process was stereospecific for the *cis*-product. Moreover, during deprotection of the aminoquinoline group, the product could be epimerized to the *trans*, or retained as the *cis* derivative. Consequently, all possible stereoisomers could be readily obtained [e.g., (–)-**170** and (+)-**171**, Scheme 27c].

With this method, the synthesis of BRD3914 was achieved in 10% overall yield from azetidine-2-carboxylic acid (+)-**166**. The key arylation step using 1-bromo-4-iodobenzene was achieved on a 10-g scale to afford (–)-**168f**, which was converted into (–)-**170** (Scheme 27c). Boc deprotection and reductive alkylation, followed by intramolecular amidation gave bicycle (–)-**172** (Scheme 28). $Ru_3(CO)_{12}$ and 1,1,3,3-tetramethyldisiloxane (TMDS) were used to reduce the lactam to the secondary amine, which was trapped in situ with 4-methoxyphenyl isocyanate. Finally, a palladium-catalyzed alkynylation gave BRD3914.

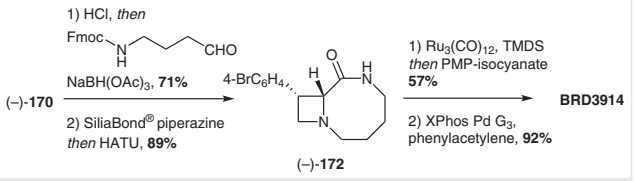

Scheme 28 Final steps in the synthesis of BRD3914

The Schreiber group reported similar conditions to effect C–H arylation of pyroglutamic acid derivatives.[72] The use of 20 mol% dibenzyl phosphate additive and cyclopentyl methyl ether (CPME) as the solvent promoted the *syn*-arylation of substrates **173** (Scheme 29). The reaction was successful in the presence Cbz and PMP *N*-protecting groups, but failed with either *N*-Boc or a free N–H lactam. Directing group removal was successfully achieved under Maulide's ozonolytic protocol.[65]

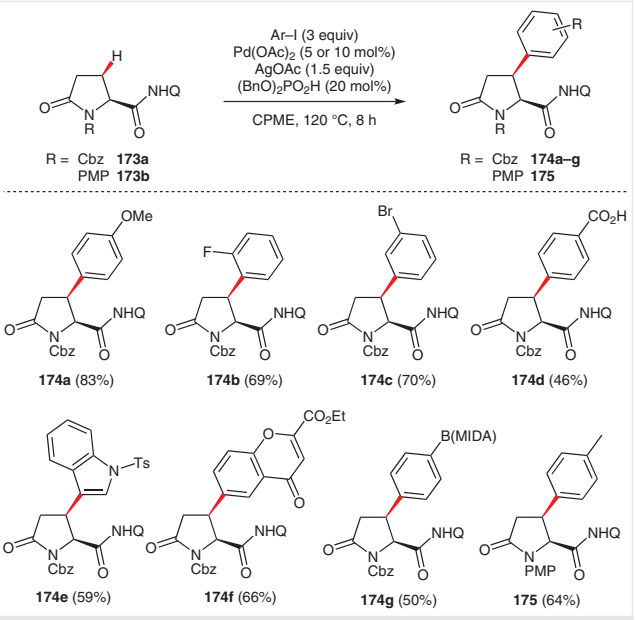

Scheme 29 Pd-catalyzed arylation of pyroglutamic acid derivatives; products isolated as single enantiomers and diastereomers

Babu and Parella described the Pd-catalyzed arylation of tetrahydrofurans at the 3-position with various aryl iodides (Table 21).[73] The use of a C(2)-linked 8-AQ auxiliary was critical for the reaction, as other directing groups were inactive. 2,3-Disubstituted tetrahydrofuran derivatives **178** were synthesized in good yields and excellent *cis*-diastereoselectivity using 10 mol% $Pd(OAc)_2$ and 4 equiv of aryl iodide. Enantioenriched substrates reacted under these conditions without significant racemization. The same conditions also enabled C(sp^3)–H functionalization of 1,4-benzodioxane derivative **177** with *cis*-selectivity. Despite the reduced steric bulk compared to the *N*-protected pyrrolidine ring, AQ removal continued to be challenging on these O-heterocycles. Carboxamide hydrolysis was achieved under strong acidic conditions, by treatment with triflic acid at 100 °C. This afforded the corresponding *cis*-carboxylic acids, importantly without any detectable epimerization.

Bull and co-workers also reported related conditions for tetrahydrofuran arylation.[61] Increasing the concentration proved beneficial for the reaction of *N*-(quinolin-8-yl)tetrahydrofuran-2-carboxamide **180** with aryl iodides and best results were achieved in absence of solvent. This enabled the use of lower catalyst and iodide loadings (Scheme 30a).

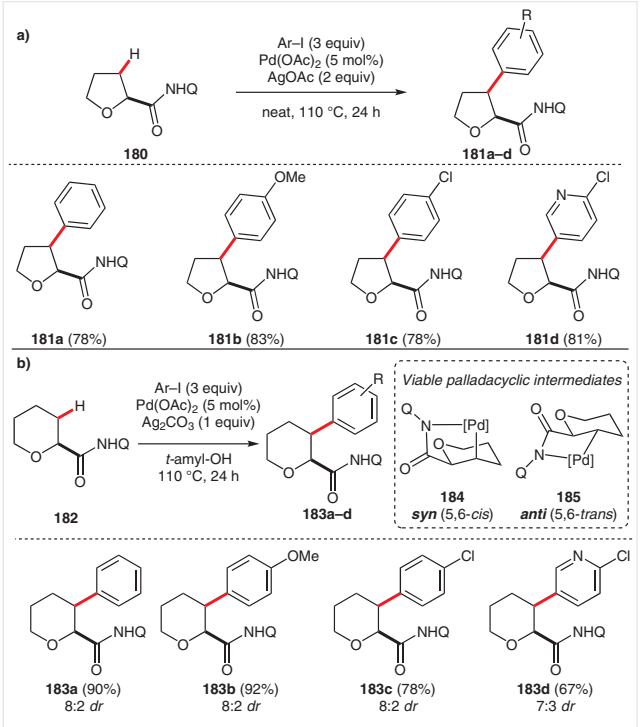

Scheme 30 (a) Pd-catalyzed arylation of *N*-(quinolin-8-yl)tetrahydrofuran-2-carboxamide under neat conditions; products isolated as single *cis*-diastereomer. (b) Pd-catalyzed arylation of *N*-(quinolin-8-yl)tetrahydropyran-2-carboxamide; major *cis*-diastereomer shown.

Table 21 AQ-Enabled C(3)–H Arylation of Tetrahydrofuran and 1,4-Benzodioxane Rings

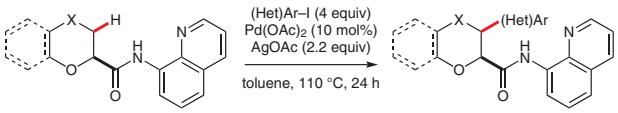

Substrate	Product[a]			Yield (ee) (%)
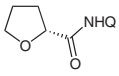	**176**	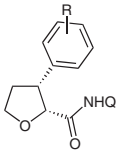	R = 4-OMe 4-COMe 4-CN 4-Br-3-F	**178a** 71 (95) **178b** 81 (97) **178c** 78 (93) **178d** 65 (81)
		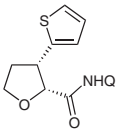		**178e** 81 (99)
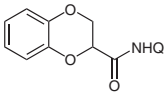	**177**	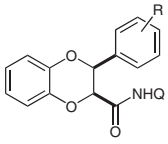	R = 4-OMe 4-Br 3,4-Me	**179a** 81 **179b** 83 **179c** 82
		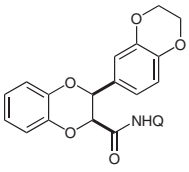		**179d** 82%

[a] Products isolated as single *cis*-diastereomers. Q = quinolin-8-yl.

N-(Quinolin-8-yl)tetrahydropyran-2-carboxamide **182** was also successfully arylated at C(3) using 1 equiv of Ag_2CO_3 and *tert*-amyl alcohol as the solvent (Scheme 30b).[61] However, unlike for pyrrolidine and tetrahydrofuran rings, a mixture of *cis*- and *trans*-configured products **183** was observed in this case (dr ranging from 7:3 to 8:2, *cis*/*trans*). The diastereomeric ratio remained identical when resubjecting the purified products to the reaction conditions. This excluded a base-mediated epimerization and suggested a *trans*-configured palladacycle **185**, formed alongside the expected *cis*-intermediate **184**, leading to the minor *trans*-product.

The C(sp^3)–H arylation of 3-deoxyglycosyl-2-carboxamides was reported by Messaoudi, Gandon, and co-workers in 2018.[74] Despite the high steric congestion, arylation of these carbohydrate substrates was successfully achieved exploiting the strong directing ability of 8-aminoquinoline. A high loading of Pd catalyst (20 mol%) was required, likely due to the presence of many coordinating groups able to compete with the AQ auxiliary. As a consequence, only fully protected glycosides proved to be suitable substrates. Under optimized conditions, various 3-arylated β-glycosides **189**–**191** were synthesized in moderate to good yields with exclusive 2,3-*trans*-configuration (Scheme 31a).

This switch in diastereoselectivity, compared to previously studied heterocyclic systems, was investigated through in-depth mechanistic studies.[74] *trans*-Configured palladacycle **192** was isolated with a stoichiometric amount of $Pd(OAc)_2$, indicating preferential C(3)–H activation occurring at the equatorial position. This tendency is supported by computational evaluation of both *cis*- and *trans*-CMD transition states (Scheme 31b). The lowest energy barrier is associated to the *trans*-configured transition state **193**, where the C(4)-acetate group is equatorial. On the other hand, to minimize steric clash, *cis*-C–H activation must occur in a conformation with the C(4)-acetate in the axial position (**194**), destabilizing the transition state by 2.6 kcal/mol. In absence of any group at C(4) (i.e., for unsubstituted tetrahydropyran **182**, Scheme 30), *cis*-palladation was favored. Calculations on the overall process also indicate the CMD step to be turnover-limiting. Interestingly, when C–H arylation conditions were applied to the corresponding α-glycoside **195**, arylated compound **196** was formed as the sole product (Scheme 31c). Isolation of a *cis*-palladacycle

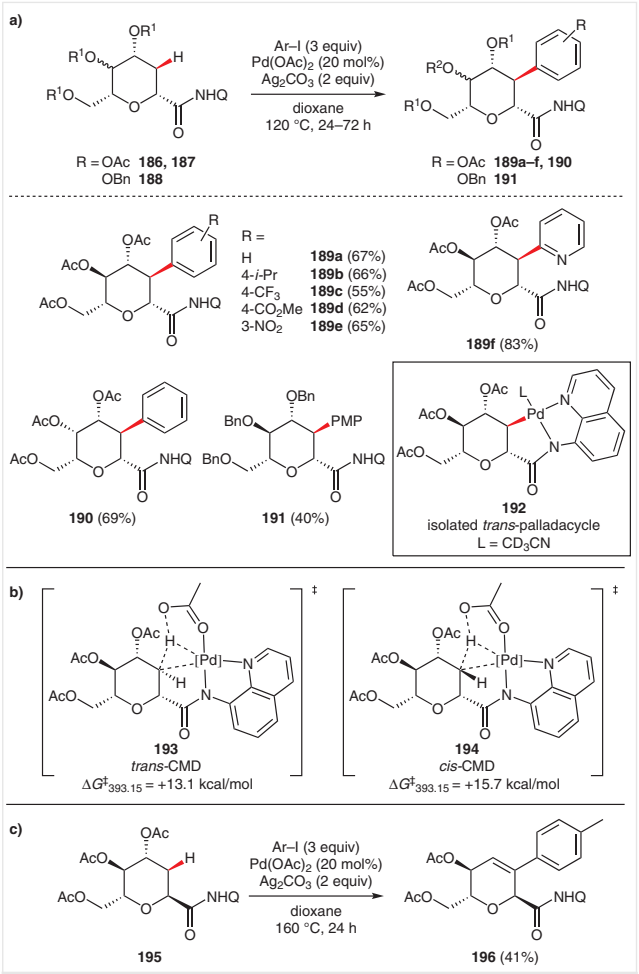

Scheme 31 (a) Diastereoselective 2,3-*trans*-arylation of β-D-glycosides directed by the 8-aminoquinoline group; products isolated as single diastereomers. (b) Calculated CMD-transition states for *trans*- and *cis*-C–H activation. (c) Arylation of an α-D-glycoside.

and additional calculations support an initial equatorial *cis*-C(3)–H arylation, now possible with an equatorial C(4)-acetate. Subsequently, a second *trans*-CMD and AcOH elimination gives the dehydrogenated product **196**.

3.1.2 Other Transformations at C(3)

There are few examples of C(sp^3)–H functionalization reactions at the C(3) position of saturated heterocycles, other than arylation. In 2013, Chen and co-workers reported the Pd-catalyzed alkylation of α-amino acids derivatives enabled by the 8-AQ directing group.[75] In this work, a single example of C(3)–H alkylation of *N*-(quinolin-8-yl)piperidine-2-carboxamide **151** was described using methyl bromoacetate (Scheme 32a). The reaction is proposed to proceed through a Pd^{II}/Pd^{IV} manifold, in which methylene C–H palladation is followed by Ag(I)-promoted S_N2-type oxidative addition of the alkyl halide. In 2017, a similar C–H alkylation reaction with (iodomethyl)phosphonates was described by Yang and Yang.[76]

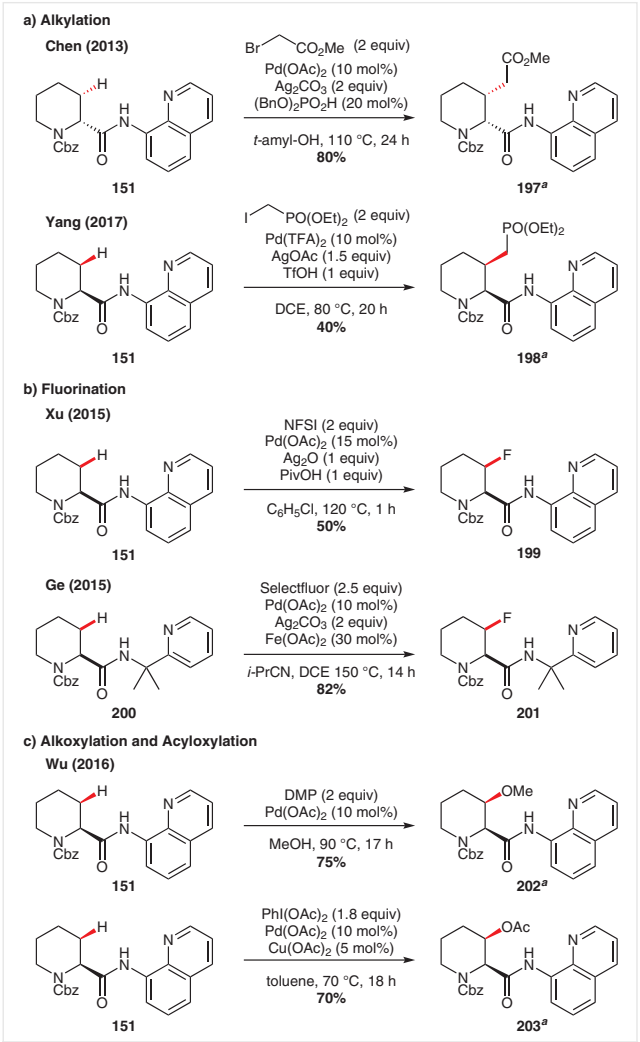

Scheme 32 Pd-catalyzed (a) alkylation, (b) fluorination, and (c) methoxylation/acetoxylation of piperidine-2-carboxamides; products isolated as single *cis*-diastereomers. [a] Isolated as single enantiomers.

β-C–H Fluorination of carboxylic acid derivatives was independently reported by Xu and co-workers[77] and Ge and co-workers,[78] including isolated examples of piperidine C(3) functionalization (Scheme 32b). NFSI and Selectfluor were used as electrophilic fluorine sources in the presence of *N*-quinolin-8-yl and *N*-[2-(2-pyridyl)isopropyl] (PIP)[15a] amide auxiliaries, respectively. In both cases, silver(I) salts are proposed to facilitate oxidative addition and formation of a Pd^{IV}–F complex. This then undergoes reductive elimination to form the new C–F bond. A stoichiometric amount of pivalic acid (PivOH) was required in combination with NFSI to substitute the $N(SO_2Ph)_2$ ligand on palladium and prevent competing C–N bond-forming reductive elimination.

During their studies on piperidine arylation, Wu, Cao, and co-workers also described the use of high-valent iodine reagents to promote the Pd-catalyzed alkoxylation and acyloxylation of the same ring.[66a] Reaction with Dess–Martin periodinane (DMP) in MeOH afforded methoxylated piperidine **202** in high yield (Scheme 32c). When using 1-methoxy-1,2-benziodoxole as the oxidant, acyloxylation was preferentially observed. Piperidine C(3)–H acetoxylation was achieved with 1.8 equiv of (diacetoxyiodo)benzene giving 2,3-disubstituted derivative **203** in 70% yield.

Wu, Cao, and co-workers then also developed a Pd-catalyzed intramolecular amination of methylene C–H bonds as a strategy to access β-lactams from various carboxamides.[79] The use of electron-poor pentafluoroiodobenzene as an oxidant was essential to promote selective C–N bond formation, from a high-valent Pd^{IV} species. Linear and cyclic carboxamides could be aminated, including pyrrolidine and piperidine derivatives **204** (Scheme 33). Notably, oxidative removal of the 5-MeO-quinoline group and Cbz deprotection afforded various N–H diazabicyclic β-lactams of interest as a core structure of β-lactamase inhibitors.[80]

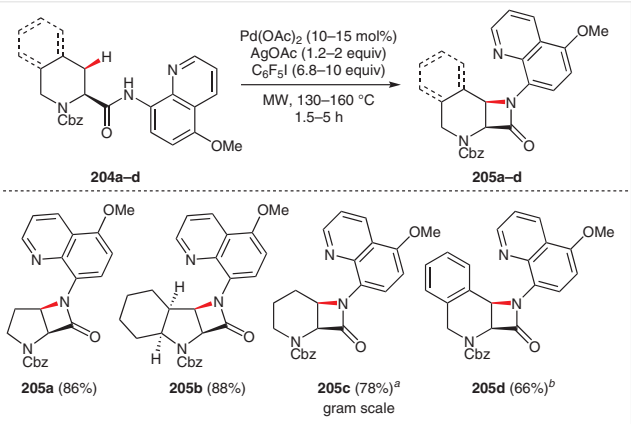

Scheme 33 Pd-catalyzed intramolecular amination of pyrrolidine- and piperidine-2-carboxamide derivatives; products isolated as single enantiomers. [a] 1,1,2,2-Tetrachloroethane was added as co-solvent. [b] C_6F_5I (37 equiv).

3.2 C–H Functionalization at C(3), C(4), and C(5): Directing Groups at C(4) and C(3)

C(sp^3)–H Functionalization of saturated heterocycles using directing groups at either C(3) or C(4) is much less explored than with N or C(2) auxiliaries. Isolated early examples of C(3) functionalization of *N*-(perfluoro-4-tolyl)tetrahydropyran-4-carboxamide **206** were reported by the Yu group in 2012, in the broader context of ligand-enabled methylene C–H arylation and alkynylation reactions (Scheme 34). The use of quinoline ligand **207** was essential to enable C–H arylation, by Pd^{II}/Pd^{IV} catalysis.[81] Simultaneous coordination of the ligand and the *N*-arylamide auxiliary to the Pd^{II} center promoted C–H bond cleavage and avoided subsequent β-hydride elimination. Monoarylated tetrahydropyran **208** was isolated in good yield as a mixture of *cis*- and *trans*-isomers (6:1 dr, *cis*/*trans*). Preferential monofunctionalization and complete *cis*-selectivity was also observed for the Pd-catalyzed alkynylation of tetrahydropyran **206** with TIPS-ethynyl bromide.[82] The reaction was enabled by an adamantyl-substituted NHC ligand (IAd·HBF_4) and likely proceeds through a Pd^0/Pd^{II} redox cycle, where oxidative addition of the alkynyl halide gives an [alkynylPd(II)L_n] species, which is proposed to activate and alkynylate the β-C–H bond.

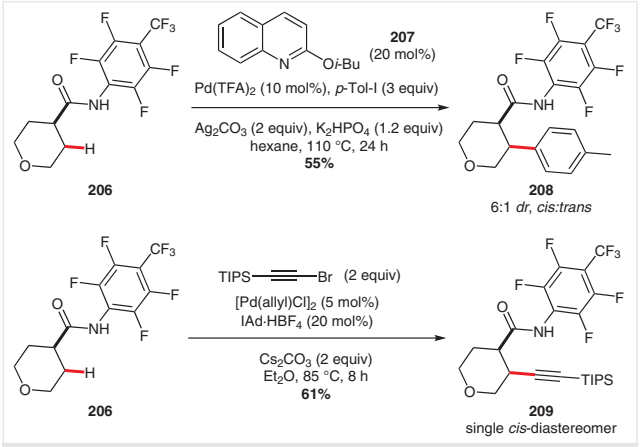

Scheme 34 Early examples of ligand-enabled C–H functionalization of tetrahydropyran-4-carboxamide involving Pd^{II}/Pd^{IV} or Pd^0/Pd^{II} catalysis

Yu, Stamos, and co-workers also reported carbene ligands to enable C–H arylation of tetrahydropyran and piperidine derivatives, including some examples with the directing group at C(4) and C(3) positions (Table 22).[69] Lower yields and reduced stereoselectivity were obtained in comparison with the C(2)-linked auxiliary (cf. Table 20). Piperidine-4-carboxamide **210a** was arylated in good yield, while lower reactivity was observed for tetrahydropyran derivative **206**. This likely results from an outcompeting bidentate coordination of the substrate to the catalyst in a boat conformation. In both cases, only monoarylated products **208** and **213a** were isolated, although with poor stereoselectivity. Higher *cis*-selectivity was observed for the analogous tetrahydrothiopyran dioxide derivative **210b**, further indicating the strong effect of the heteroatom and/or protecting groups on the reaction outcome.

Table 22 Pd-Catalyzed C–H Arylation of Six-Membered Saturated Heterocycles Using the Directing Group at C(4) and C(3)

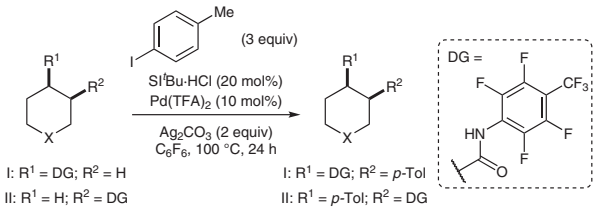

Substrate				Product[a]			Yield (%)	dr[b]
I		X = O NCOCF$_3$ SO$_2$	**206** **210a** **210b**	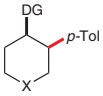	X = O NCOCF$_3$ SO$_2$	**208** **213a** **213b**	37 57 62	1:1 3:2 7:1
II		X = O NCOCF$_3$	**211a** **211b**		X = O NCOCF$_3$	**214a** **214b**	72 66	3:2 1:1
II	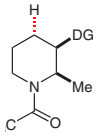		**212**	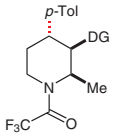		**215**	74	>1:20

[a] Major diastereomer shown.
[b] *cis*/*trans*.

The same conditions also effected the arylation of tetrahydropyran derivative **211a** with a C(3) directing group, providing 3,4-disubstituted derivative **214a** in high yield (3:2 dr, *cis*/*trans*). Notably, arylation occurred exclusively at C(4), despite the presence of a weaker C(2)–H bond. This is ascribed to a repulsion from the heteroatom lone pairs of electrons, hindering the formation of a partial negative charge on the α-carbon during the C–H activation step. Similar C(4) regioselectivity was observed for piperidine-3-carboxamide **211b**, which gave a 1:1 mixture of *cis*- and *trans*-4-arylated products. Interestingly, introducing a *cis*-methyl substituent at C(2) in **212** afforded 4-arylated piperidine **215** in high yield as a single *trans*-diastereomer. This stereoselectivity switch likely derives from the 2-methyl group occupying the α-axial position in the reactive conformation, hindering activation of the *cis*-axial C(4)–H bond.

In 2018, Bull and co-workers described a general method for the Pd-catalyzed C(4)–H arylation of pyrrolidine and piperidine rings with aryl iodides using a C(3) directing group.[83] Despite the more activated nature of the α-C–H bond, preferential C(4) arylation was achieved using an AQ amide auxiliary with *N*-Boc or *N*-Cbz protecting groups. This was ascribed to the steric preference for the less hindered C(4) position. Optimum conditions were silver-free and involved the use of K_2CO_3 as a base in combination with PivOH. Under these conditions, 3,4-disubstituted pyrrolidine derivatives **217** and **218** were synthesized in moderate to good yields and high regioselectivity (Table 23). The reaction was highly tolerant of varied functionalities in the coupling partner with higher yields observed for more electron-rich aryl iodides.

Importantly, the reaction proceeded with excellent *cis*-diastereoselectivity, and the use of enantiopure substrates afforded enantiopure *cis*-products. Epimerization to the *trans*-4-arylated pyrrolidine could be promoted under basic conditions with complete preservation of ee, demonstrating the potential to access all possible stereoisomers. Divergent removal of the directing group was accomplished to afford various biologically relevant building blocks. Boc protection furnished activated amides **220**, which were then converted into carboxylic acid, amide, ester, and alcohol containing derivatives **221**–**224** (Scheme 35). Each set of conditions was optimized to minimize product epimerization, preserving the starting *cis*-configuration. Alternatively, *trans*-carboxylic acid derivative **219** was directly obtained by hydrolysis/epimerization of arylated pyrrolidine **217a** with NaOH. Subsequent treatment with trifluoroacetic acid afforded the corresponding unnatural amino acid in high yield.

The same arylation conditions were also suitable for analogous *N*-(quinolin-8-yl)piperidine-3-carboxamide **225**, resulting in identical C(4) regioselectivity (Scheme 36). Formation of a minor *trans*-arylated product was observed in this case (6:4 to 7:3 dr, *cis*/*trans*). No epimerization was found resubjecting the major *cis*-derivative **226** to the stan-

Table 23 Stereoselective Pd-Catalyzed C(4)–H Arylation of *N*-(Quinolin-8-yl)pyrrolidine-3-carboxamides with Aryl Iodides

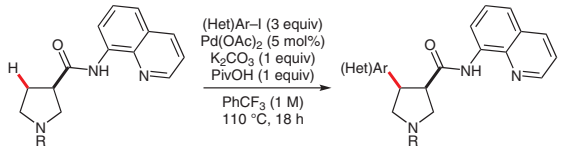

Ar–I		Product	Yield (%)[a]
	X =		
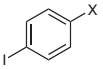	OMe	**217a**	64
	OMe	**218a**	67
	Me	**217b**	55
	Br	**217c**	45
	CO_2Et	**217d**	31
	NHBoc	**218b**	54
	SMe	**217e**	55
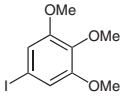		**217f**	58
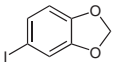		**217g**	59
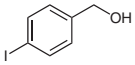		**217h**	35
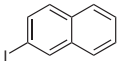		**218c**	52
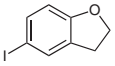		**218d**	63
		**218e**	56
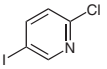		**218f**	23
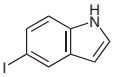		**218g**	60

[a] Products isolated as single *cis*-diastereomers.

dard arylation conditions, suggesting the *trans*-isomer **227** derived from a *trans*-configured palladacycle intermediate **229**, formed alongside the expected *cis*-intermediate **228**.

The synthetic utility of the arylation protocol was demonstrated in the stereocontrolled formal synthesis of antidepressant drug (–)-paroxetine (**236**) from readily available *N*-Boc (*R*)-nipecotic acid **230** (Scheme 37).[84] Stereospecific C(4)–H arylation was followed by selective C(3) epimerization and reductive directing group removal to afford key alcohol intermediate (–)-**235** as a single enantiomer. Notably, isomerization of the major *cis*-arylated

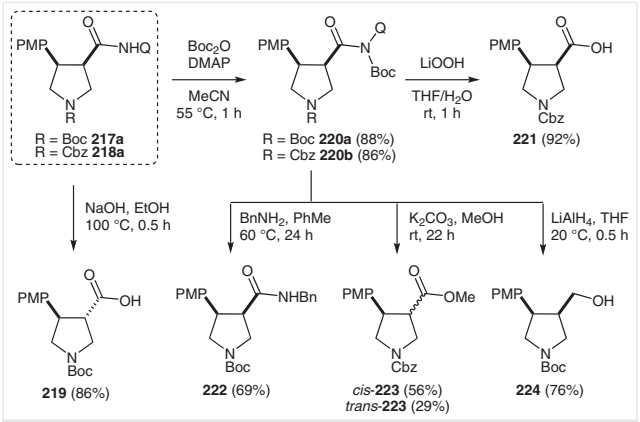

Scheme 35 Divergent removal of the aminoquinoline directing group

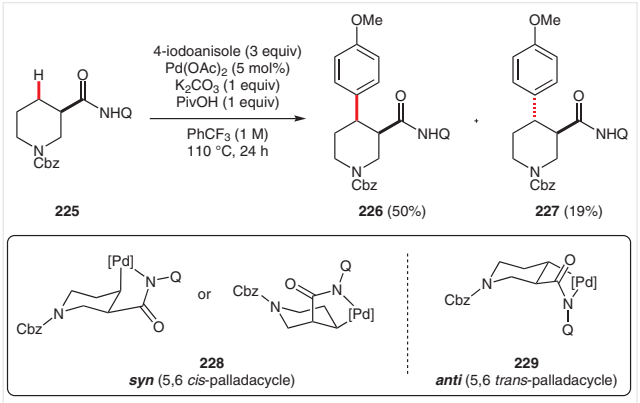

Scheme 36 Pd-catalyzed arylation of an *N*-(quinolin-8-yl)piperidine-3-carboxamide derivative

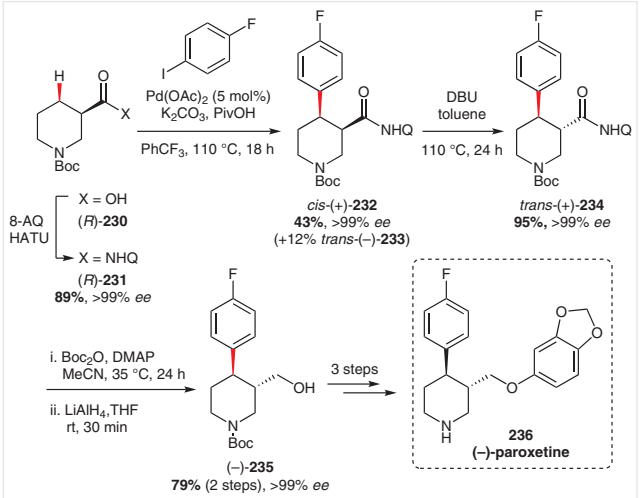

Scheme 37 Stereocontrolled formal synthesis of (–)-paroxetine via piperidine C(4)–H arylation

product (+)-**232** with DBU gave *trans*-(+)-**234**, the enantiomer of the minor *trans*-derivative (–)-**233** formed in the C–H arylation step (not shown). This further supported the proposed *trans*-palladacycle **229** as an intermediate in the C–H functionalization of the piperidine ring.

The use of a picolinamide auxiliary[11b] was reported by the Maes group to effect the diastereoselective C(5)–H arylation of piperidin-3-amine derivatives.[85] The inverted amide-directing group promoted γ-arylation, referring to the native amino functionality, with the reaction proceeding through a bridged five-membered palladacycle **239** (Table 24). The geometric constrains of this intermediate accounted for the complete *cis*-stereoselectivity observed. The piperidine system proved much less reactive than the corresponding cyclohexylamine derivative,[86] with a significant effect played by the *N*-protecting group; the best results were obtained with an *N*-Boc substituent. The use of a catalytic amount of 2,6-dimethylbenzoic acid additive in combination with solvent-free conditions and high loading of aryl iodide (6–8 equiv) was required to achieve optimal yields. The excess aryl iodide could generally be recovered during chromatographic separation. Under these conditions, various (hetero)aryl substituents were successfully installed giving *cis*-3,5-disubstituted piperidines **238** in high yields. Importantly, directing group removal was accomplished by heating with NaOH in isopropyl alcohol with full retention of the *cis*-configuration.

Table 24 Pd-Catalyzed C(5)–H Arylation of an *N*-(2-Pyridylcarbonyl)piperidine-3-amine Derivative

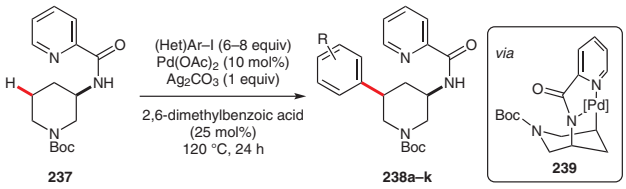

237 238a–k 239

Ar–I		Product	Yield (%)[a]
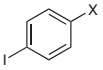	X =		
	OMe	**238a**	78
	t-Bu	**238b**	70
	H	**238c**	71
	Br	**238d**	63
	F	**238e**	70
	CF_3	**238f**	71
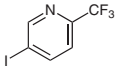		**238g**	72
	X =		
	OMe	**238h**	68
	Cl	**238i**	60
	CO_2Et	**238j**	62
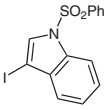		**238k**	71

[a] Products isolated as single *cis*-diastereomers.

In 2018, Maulide and co-workers reported an elegant total synthesis of (–)-quinine alkaloid **240**[87] and related analogues using a combination of directed C–H functionalization and aldol addition strategies (Scheme 38a).[88] The picolinamide directing group was used to stereoselectively arylate the quinuclidine nucleus at the C(5) position. The unfavorable α-effect of the N-atom likely accounted for the exclusive formation of 3,5-disubstituted bicycles **244**, which were obtained in high yields and diastereoselectivity (Scheme 38b). Both electron-donating and -withdrawing substituents on the aryl iodide were well tolerated, as well as more sterically congested *ortho*-substituted arenes. Although direct C–H alkenylation was not successful, the desired vinyl substituent could be introduced in four steps starting from arylated derivative (–)-**244b**. This relied on the initial oxidative cleavage of the anisole moiety into a carboxylic acid. Subsequent reduction and Wittig olefination successfully afforded the vinylated product (+)-**245**. Directing group removal under reducing conditions disclosed the starting free amine moiety, which was then oxidized to the ketone by treatment with IBX/*p*-TsOH (Scheme 38c). The next critical step in the synthesis involved installation of the second heterocyclic moiety through stereoselective aldol reaction of quinuclidone (+)-**246** with aldehyde **241**. To overcome the configurational instability of the resulting aldol product, in situ treatment with mesylhydrazine was performed. This enabled the one-pot formation of a more stable sulfonyl hydrazone in 76% yield and excellent diastereoselectivity. Final reduction afforded the desired natural product in 10 steps and 5.4% overall yield from the commercial material. The synthetic flexibility offered by the C–H arylation approach also provided access to the unnatural enantiomer (+)-quinine, and C(3)-arylated analogues of the natural alkaloid that showed an improved antimalarial profile compared to the parent compound.

The intrinsic directing ability of unprotected amines has been exploited by the Gaunt group in the Pd-catalyzed β-C–H carbonylation of aliphatic secondary amines.[89] This formed substituted β-lactams without requiring an exogenous directing group. The reaction involves initial formation of an amine-bound Pd^{II} complex followed by CO insertion into the Pd–N bond.[89a] The resulting carbamoyl–Pd(II) intermediate can then undergo methyl[89a] or methylene[89b,c] β-C–H activation (with respect to the amine) via a five-membered transition state. Interestingly, using α-tertiary amines with both a methylene and a methyl β-C–H bonds, carbonylation exclusively occurred at the methylene position, despite the higher reactivity generally shown by methyl C–H bonds.[89b] The bulky α-tertiary amine substituent is proposed to generate an unfavorable steric clash in the carbamoyl–Pd(II) complex leading to methyl C–H activation, accounting for the observed selectivity. The reaction

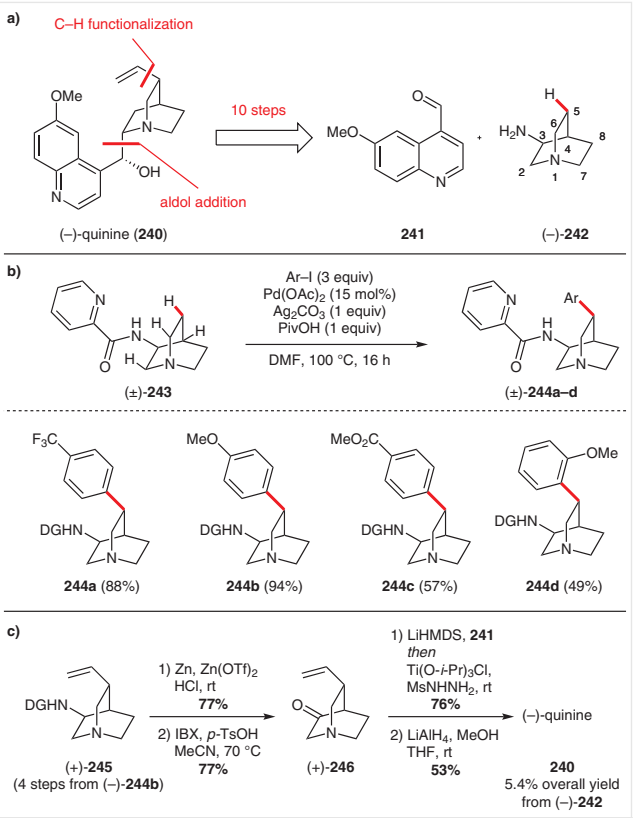

Scheme 38 (a) Stereocontrolled route to (–)-quinine. (b) Picolinamide-directed C(5)–H arylation of a quinuclidine derivative; products isolated as single diastereomers. (c) Endgame for the total synthesis of (–)-quinine.

was successful for a broad range of cyclic substrates, including few examples of saturated six-membered heterocycles, bearing a secondary amine moiety at C(3) or C(4) (Scheme 39). Bicyclic β-lactams **248** and **250** were synthesized in high yields and high C(4) selectivity (in the case of 3-aminopiperidine derivative **249**).

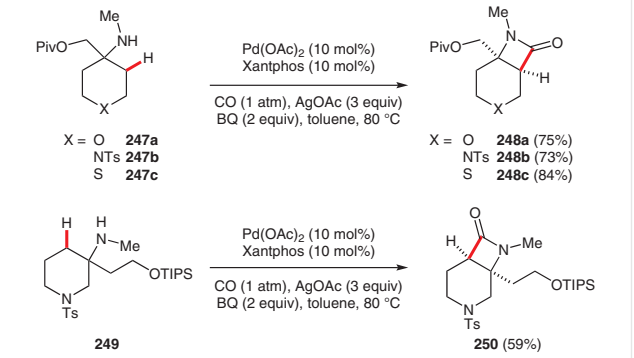

Scheme 39 Methylene C–H carbonylation of 3- and 4-amino-heterocycle derivatives

4 Transannular C–H Functionalization

Obtaining site-selective remote C–H functionalization at unactivated positions represents a distinct challenge. In 2016, Sanford and co-workers reported a Pd-catalyzed transannular C–H arylation of fused bicyclic systems, with a bidentate directing group incorporating the N-atom of the heterocycle.[90] 3-Azabicyclo[3.1.0]hexane **251** was selected as model substrate, given its prearrangement in a boat-like conformation, to position the C(4)–H bond in close proximity to the Pd^{II} center. C–H Activation formed a strained bicyclo[2.2.1]palladacycle **253** (Scheme 40). The use of CsOPiv as base was critical to prevent silver-mediated α-oxidation to an aminal product hindering the desired reactivity. Under the optimized conditions, C–H arylation with aryl iodides selectively occurred at the remote C(4) position, exclusively on the concave face, and arylated azabicycles **252** were synthesized in high yield as single diastereomers. Examples included derivative **254** as an arylated analogue of drug candidate amitifadine.[91] The directing group could be removed by treatment with SmI_2.

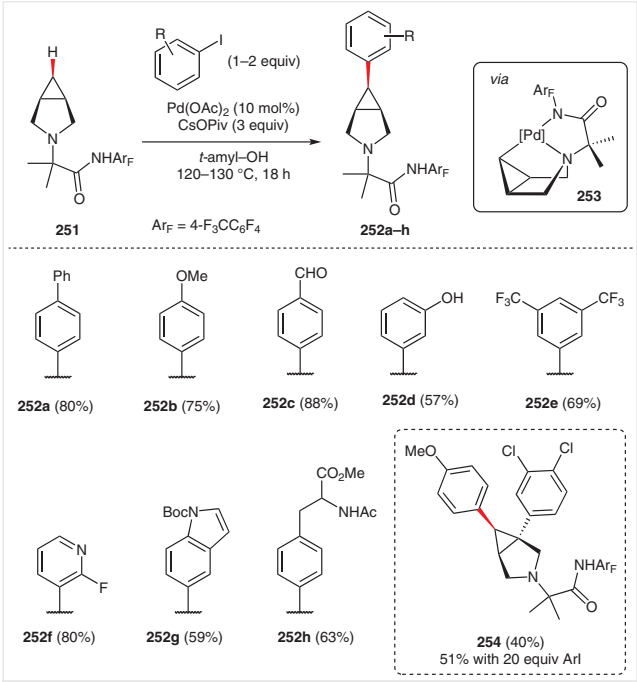

Scheme 40 Pd-catalyzed transannular C–H arylation of a 3-azabicyclo[3.1.0]hexane derivative; products isolated as single diastereomers

Remarkably, in the presence of a very large excess of the aryl iodide (used as solvent) the C(4) position of piperidine derivative **255** could be arylated. A temperature of 150 °C was required to overcome the unfavorable chair–boat isomerization of the ring to allow the concerted metalation–deprotonation transition state in the boat conformation. A

reductive workup was required to convert the aminal side-product into the desired piperidine derivative **257** (Table 25).[90]

Table 25 Pd-Catalyzed Transannular C–H Arylation of Piperidine Derivatives and Related Azabicyclic Substrates

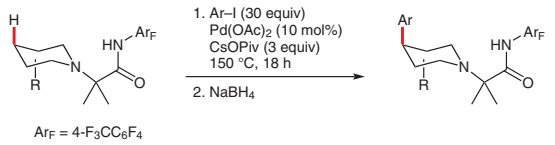

Substrate		Product		Yield (%)
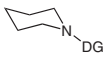	**255**	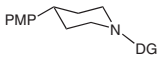	**257**	55
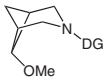	**256a**	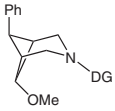	**258a**	62
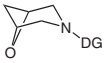	**256b**	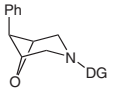	**258b**	33
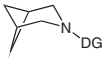	**256c**	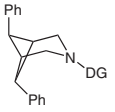	**258c**	35
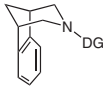	**256d**	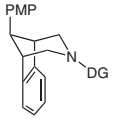	**258d**	46
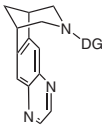	**256e**	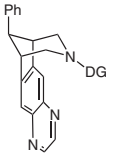	**258e**	45
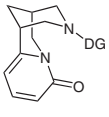	**256f**	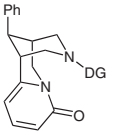	**258f**[a]	25[a]

[a] Reaction performed in *t*-amyl-OH.

These modified conditions provided a suitable platform for the functionalization of various bicyclic amines. Arylated derivatives **258**, including **258e** an analogue of the drug varenicline[92] and **258f** an analogue of natural product cytisine,[93] were successfully synthesized in moderate yield.

The mechanism of the transannular C–H arylation was extensively investigated through both DFT calculations[94] and isolation of key intermediates.[95] Based on these works, a simplified catalytic cycle is presented in Scheme 41a. Initial bidentate coordination of the substrate to Pd^{II}, through the heterocyclic N-atom and the distal tethered amide, forms complex **I**. Subsequent chair–boat isomerization orients the C(4)–H bond near the Pd^{II} center allowing C–H activation to occur via an inner sphere concerted metalation–deprotonation. The calculations indicate that this step proceeds via a concerted, but asynchronous, isomerization/CMD pathway. The energetic barrier for the C–H activation is 33.9 kcal/mol (33.0 kcal/mol using a pivalate ligand in place of acetate) suggesting this to be the turnover-limiting step. This was experimentally supported by a primary kinetic isotope effect observed for the benzo-fused azabicyclo[3.2.1]octane **256d**.[96] Higher barriers are found for the CMD occurring at the α- and β-positions of the ring, accounting for the observed γ-selectivity. The C–H activation is thermodynamically unfavorable with the bicyclic palladacycle intermediate **II** being approximately 20 kcal/mol uphill from **I**. Attempts to isolate this highly strained palladacycle were unsuccessful, but Pd^{II} complexes **259** and **260**, analogous to putative intermediate **I**, could be isolated using pyridine as a stabilizing ligand (Scheme 41b).[95]

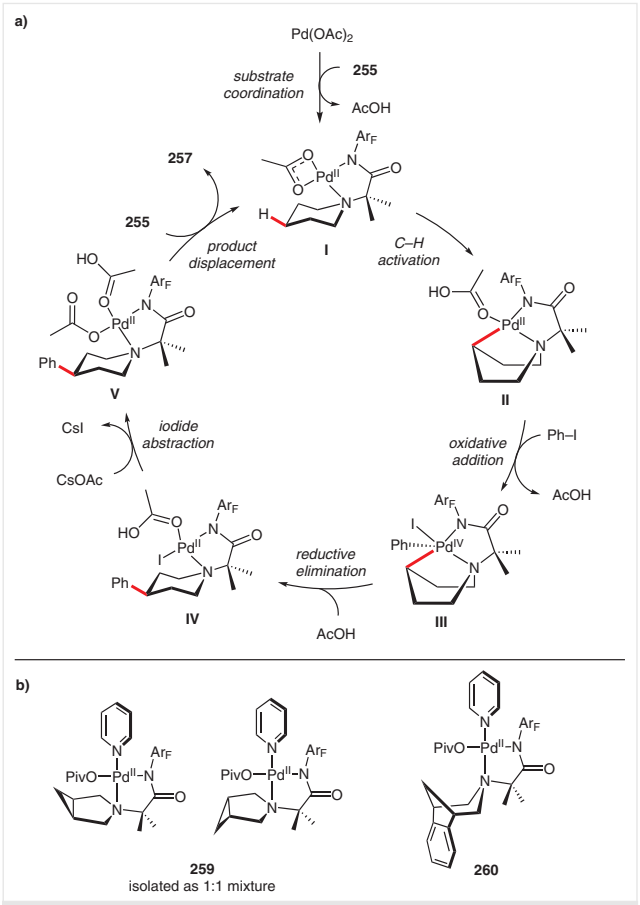

Scheme 41 (a) Proposed catalytic cycle for the transannular C–H arylation of a piperidine derivative. (b) Isolated Pd^{II} complexes.

Stoichiometric reaction of complexes **259** and **260** with iodobenzene afforded the expected arylated products in high yields. In addition, selective C(4) deuteration was observed in *tert*-butyl alcohol-d_{10}, indicating a reversible C–H activation step. Iodide coordination and oxidative addition then generates Pd^{IV} species **III**. A significantly high barrier is observed for this (32.5 kcal/mol), accounting for the large excess of aryl iodide required experimentally. In addition, the Cs salt is proposed to play an essential role in driving this step forward by sequestering the acetic acid displaced during iodide coordination. Finally, a low barrier reductive elimination is followed by cesium-mediated iodide abstraction and product displacement with a new substrate molecule.

In 2018, Sanford and co-workers described the use of quinaldic and picolinic acid ligands **261** and **264** to improve significantly the transannular C–H arylation in less reactive substrates.[96] These were found to increase the reaction rate and the longevity of the catalytic system, resulting in higher yields and broader reaction scope. This was exemplified for benzo-fused azabicyclo[3.2.1]octane **256d**, which was arylated in 81% yield upon addition of 5 mol% of ligand **261** (Scheme 42a; cf. 46% under the first generation conditions, Table 25). Notably, only 3 equiv of aryl iodide (instead of 30) were used and the reaction was performed at 120 °C instead of 150 °C.

Various arylated bicyclic amines were synthesized using this second generation approach, generally resulting in higher yields compared to the ligand-free conditions, including tropane **265** and azanorbornane **266** derivatives (Scheme 42b). Mechanistic investigations suggest the ligand is not involved in the rate-limiting C–H activation step, but rather regenerates the active catalytic species from off-cycle Pd species.

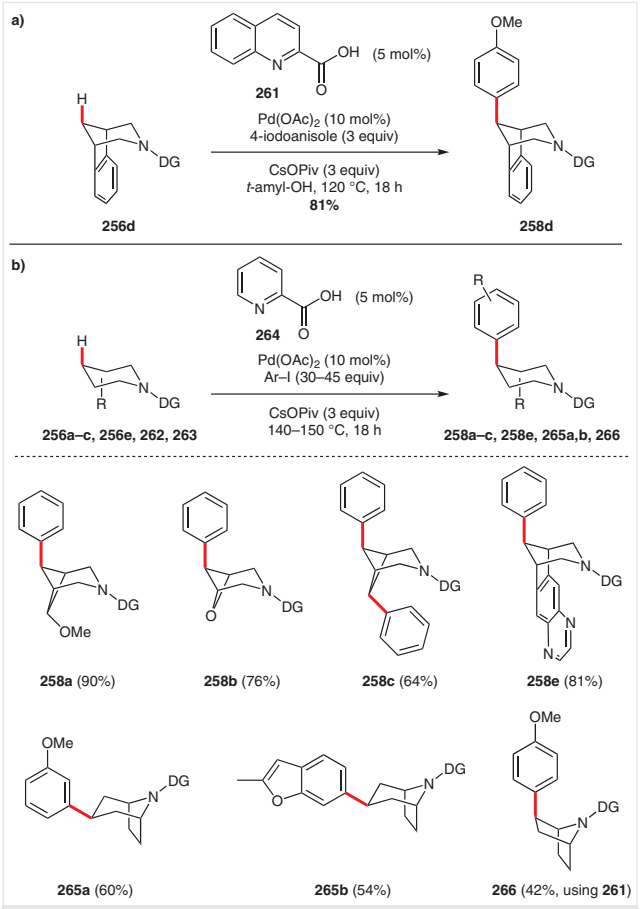

Scheme 42 Second generation transannular C–H arylation of azacycles involving the use of pyridine-2- and quinoline-2-carboxylic acid ligands

5 Conclusion

Transition metal-catalyzed C–H functionalization has been shown to be a powerful strategy for the synthesis of saturated heterocycles with varied substitution patterns. Different transition metal-catalysts have been used under distinct mechanistic scenarios to enable a range of transformations, including arylation, alkylation, and C–heteroatom bond formation. This review has focused on directed C–H functionalization of saturated heterocycles involving the formation of a discrete C–metal bond. This has been achieved often with excellent regio- and stereocontrol, providing access to different isomers of complex heterocycles. Indeed, many of the derivatives that can be accessed rapidly would present a significant challenge to prepare by other methods. This is particularly true for the enantioenriched derivatives, where C–H functionalization can take advantage of inexpensive and readily available enantiopure substrates, including chiral pool materials. In many cases, the synthesis of biologically relevant molecules demonstrated the high potential of these protocols for applications in medicinal chemistry and drug discovery programs. However, there is still considerable scope for new and improved transformations.

Important progress has been made in α-C–H functionalization with N-linked directing groups. Most recent developments have achieved this enantioselectively with chiral ligands. Methods for C–H functionalization at unactivated positions are more limited, particularly for reactions occurring at C–H bonds that are more remote from the directing group. High substrate specificity for the reaction conditions is generally observed due to the different effect of the (protected) heteroatoms on the conformation of the ring and of their different interaction with the catalytic system. Similarly, the diastereoselectivity is commonly controlled by the substrate requirements. Enantioselective functionalization at positions remote from the heteroatom has not been achieved thus far. Finally, selective strategies for C–H functionalization without the requirement for covalently linked directing groups, or indeed protecting groups, remain in

great demand for efficient synthetic sequences and late-stage functionalization processes.

Future advances in the field, solving these important limitations, will significantly expand the portfolio of synthetic tools available to synthetic and medicinal chemists, providing efficient access to diverse libraries of highly valuable heterocyclic compounds.

Funding Information

We gratefully acknowledge The Royal Society for University Research Fellowship (UF140161 to J.A.B.), URF appointed grant (RG150444) and URF enhancement grant (RGF\EA\180031).

References

(1) (a) Taylor, R. D.; MacCoss, M.; Lawson, A. D. G. *J. Med. Chem.* **2014**, *57*, 5845. (b) Aldeghi, M.; Malhotra, S.; Selwood, D. L.; Chan, A. W. E. *Chem. Biol. Drug Des.* **2014**, *83*, 450. (c) Vitaku, E.; Smith, D. T.; Njardarson, J. T. *J. Med. Chem.* **2014**, *57*, 10257.

(2) (a) O'Hagan, D. *Nat. Prod. Rep.* **2000**, *17*, 435. (b) Saleem, M.; Kim, H. J.; Ali, M. S.; Lee, Y. S. *Nat. Prod. Rep.* **2005**, *22*, 696. (c) Galliford, C. V.; Scheidt, K. A. *Angew. Chem. Int. Ed.* **2007**, *46*, 8748. (d) Lorente, A.; Lamariano-Merketegi, J.; Albericio, F.; Álvarez, M. *Chem. Rev.* **2013**, *113*, 4567.

(3) Blakemore, D. C.; Castro, L.; Churcher, I.; Rees, D. C.; Thomas, A. W.; Wilson, D. M.; Wood, A. *Nat. Chem.* **2018**, *10*, 383.

(4) (a) Lovering, F.; Bikker, J.; Humblet, C. *J. Med. Chem.* **2009**, *52*, 6752. (b) Lovering, F. *Med. Chem. Commun.* **2013**, *4*, 515. (c) Nadin, A.; Hattotuwagama, C.; Churcher, I. *Angew. Chem. Int. Ed.* **2012**, *51*, 1114. (d) Murray, C. W.; Rees, D. C. *Angew. Chem. Int. Ed.* **2016**, *55*, 488.

(5) (a) Godula, K.; Sames, D. *Science* **2006**, *312*, 67. (b) Wencel-Delord, J.; Dröge, T.; Liu, F.; Glorius, F. *Chem. Soc. Rev.* **2011**, *40*, 4740. (c) McMurray, L.; O'Hara, F.; Gaunt, M. J. *Chem. Soc. Rev.* **2011**, *40*, 1885. (d) Yamaguchi, J.; Yamaguchi, A. D.; Itami, K. *Angew. Chem. Int. Ed.* **2012**, *51*, 8960. (e) Wencel-Delord, J.; Glorius, F. *Nat. Chem.* **2013**, *5*, 369. (f) Wang, W.; Lorion, M. M.; Shah, J.; Kapdi, A. R.; Ackermann, L. *Angew. Chem. Int. Ed.* **2018**, *57*, 14700.

(6) (a) Boutadla, Y.; Davies, D. L.; Macgregor, S. A.; Poblador-Bahamonde, A. I. *Dalton Trans.* **2009**, 5820. (b) Lapointe, D.; Fagnou, K. *Chem. Lett.* **2010**, *39*, 1118. (c) Ackermann, L. *Chem. Rev.* **2011**, *111*, 1315. (d) Davies, D. L.; Macgregor, S. A.; McMullin, C. L. *Chem. Rev.* **2017**, *117*, 8649.

(7) For recent selected examples of late-stage C–H functionalization see: (a) Larsen, M. A.; Hartwig, J. F. *J. Am. Chem. Soc.* **2014**, *136*, 4287. (b) Wang, W.; Lorion, M. M.; Martinazzoli, O.; Ackermann, L. *Angew. Chem. Int. Ed.* **2018**, *57*, 10554. (c) Simonetti, M.; Cannas, D. M.; Just-Baringo, X.; Vitorica-Yrezabal, I. J.; Larrosa, I. *Nat. Chem.* **2018**, *10*, 724.

(8) (a) Alberico, D.; Scott, M. E.; Lautens, M. *Chem. Rev.* **2007**, *107*, 174. (b) Ackermann, L.; Vicente, R.; Kapdi, A. R. *Angew. Chem. Int. Ed.* **2009**, *48*, 9792. (c) Ping, L.; Chung, D. S.; Bouffard, J.; Lee, S. *Chem. Soc. Rev.* **2017**, *46*, 4299. (d) Mihai, M. T.; Genov, G. R.; Phipps, R. J. *Chem. Soc. Rev.* **2018**, *47*, 149.

(9) (a) Baudoin, O. *Chem. Soc. Rev.* **2011**, *40*, 4902. (b) Dastbaravardeh, N.; Christakakou, M.; Haider, M.; Schnürch, M. *Synthesis* **2014**, *46*, 1421. (c) Bruneau, C. In *Ruthenium in Catalysis*; Dixneuf, P. H.; Bruneau, C., Ed.; Springer: Cham, **2014**, 195. (d) He, J.; Wasa, M.; Chan, K. S. L.; Shao, Q.; Yu, J.-Q. *Chem. Rev.* **2017**, *117*, 8754. (e) Chu, J. C. K.; Rovis, T. *Angew. Chem. Int. Ed.* **2018**, *57*, 62.

(10) (a) Rouquet, G.; Chatani, N. *Angew. Chem. Int. Ed.* **2013**, *52*, 11726. (b) Zhang, M.; Zhang, Y.; Jie, X.; Zhao, H.; Li, G.; Su, W. *Org. Chem. Front.* **2014**, *1*, 843. (c) Chen, Z.; Wang, B.; Zhang, J.; Yu, W.; Liu, Z.; Zhang, Y. *Org. Chem. Front.* **2015**, *2*, 1107. (d) Daugulis, O.; Roane, J.; Tran, L. D. *Acc. Chem. Res.* **2015**, *48*, 1053. (e) Xu, Y.; Dong, G. *Chem. Sci.* **2018**, *9*, 1424. (f) Sambiagio, C.; Schönbauer, D.; Blieck, R.; Dao-Huy, T.; Pototschnig, G.; Schaaf, P.; Wiesinger, T.; Zia, M. F.; Wencel-Delord, J.; Besset, T.; Maes, B. U. W.; Schnürch, M. *Chem. Soc. Rev.* **2018**, *47*, 6603.

(11) (a) Zaitsev, V. G.; Shabashov, D.; Daugulis, O. *J. Am. Chem. Soc.* **2005**, *127*, 13154. (b) Shabashov, D.; Daugulis, O. *J. Am. Chem. Soc.* **2010**, *132*, 3965.

(12) (a) Giri, R.; Maugel, N.; Li, J.-J.; Wang, D.-H.; Breazzano, S. P.; Saunders, L. B.; Yu, J.-Q. *J. Am. Chem. Soc.* **2007**, *129*, 3510. (b) Shi, B.-F.; Maugel, N.; Zhang, Y.-H.; Yu, J.-Q. *Angew. Chem. Int. Ed.* **2008**, *47*, 4882.

(13) For selected examples see: (a) Feng, Y.; Chen, G. *Angew. Chem. Int. Ed.* **2010**, *49*, 958. (b) Gutekunst, W. R.; Gianatassio, R.; Baran, P. S. *Angew. Chem. Int. Ed.* **2012**, *51*, 7507. (c) Roman, D. S.; Charette, A. B. *Org. Lett.* **2013**, *15*, 4394. (d) Yan, S.-B.; Zhang, S.; Duan, W.-L. *Org. Lett.* **2015**, *17*, 2458. (e) Chapman, L. M.; Beck, J. C.; Wu, L.; Reisman, S. E. *J. Am. Chem. Soc.* **2016**, *138*, 9803. (f) Zhang, X.; Lu, G.; Sun, M.; Mahankali, M.; Ma, Y.; Zhang, M.; Hua, W.; Hu, Y.; Wang, Q.; Chen, J.; He, G.; Qi, X.; Shen, W.; Liu, P.; Chen, G. *Nat. Chem.* **2018**, *10*, 540.

(14) For reviews see: (a) Engle, K. M.; Mei, T.-S.; Wasa, M.; Yu, J.-Q. *Acc. Chem. Res.* **2012**, *45*, 788. (b) Yang, Y.-F.; Hong, X.; Yu, J.-Q.; Houk, K. N. *Acc. Chem. Res.* **2017**, *50*, 2853. For selected recent examples see: (c) Chu, L.; Xiao, K.-J.; Yu, J.-Q. *Science* **2014**, *346*, 451. (d) Chan, K. S. L.; Fu, H.-Y.; Yu, J.-Q. *J. Am. Chem. Soc.* **2015**, *137*, 2042. (e) Chen, G.; Gong, W.; Zhuang, Z.; Andrä, M. S.; Chen, Y.-Q.; Hong, X.; Yang, Y.-F.; Liu, T.; Houk, K. N.; Yu, J.-Q. *Science* **2016**, *353*, 1023. (f) Wu, Q.-F.; Shen, P.-X.; He, J.; Wang, X.-B.; Zhang, F.; Shao, Q.; Zhu, R.-Y.; Mapelli, C.; Qiao, J. X.; Poss, M. A.; Yu, J.-Q. *Science* **2017**, *355*, 499. (g) He, J.; Shao, Q.; Wu, Q.; Yu, J.-Q. *J. Am. Chem. Soc.* **2017**, *139*, 3344. (h) Shen, P.-X.; Hu, L.; Shao, Q.; Hong, K.; Yu, J.-Q. *J. Am. Chem. Soc.* **2018**, *140*, 6545.

(15) For selected examples see: (a) Chen, F.-J.; Zhao, S.; Hu, F.; Chen, K.; Zhang, Q.; Zhang, S.-Q.; Shi, B.-F. *Chem. Sci.* **2013**, *4*, 4187. (b) He, G.; Zhang, S.-Y.; Nack, W. A.; Li, Q.; Chen, G. *Angew. Chem. Int. Ed.* **2013**, *52*, 11124. (c) Rodríguez, N.; Romero-Revilla, J. A.; Fernández-Ibáñez, M. Á.; Carretero, J. C. *Chem. Sci.* **2013**, *4*, 175. (d) Fan, M.; Ma, D. *Angew. Chem. Int. Ed.* **2013**, *52*, 12152. (e) Xu, Y.; Yan, G.; Ren, Z.; Dong, G. *Nat. Chem.* **2015**, *7*, 829. (f) Zhang, Y.-F.; Zhao, H.-W.; Wang, H.; Wei, J.-B.; Shi, Z.-J. *Angew. Chem. Int. Ed.* **2015**, *54*, 13686. (g) Knight, B. J.; Rothbaum, J. O.; Ferreira, E. M. *Chem. Sci.* **2016**, *7*, 1982.

(16) For a recent review, see: (a) St John-Campbell, S.; Bull, J. A. *Org. Biomol. Chem.* **2018**, *16*, 4582. For selected examples see: (b) Zhang, F.-L.; Hong, K.; Li, T.-J.; Park, H.; Yu, J.-Q. *Science* **2016**, *351*, 252. (c) Yang, K.; Li, Q.; Liu, Y.; Li, G.; Ge, H. *J. Am. Chem. Soc.* **2016**, *138*, 12775. (d) Wu, Y.; Chen, Y.-Q.; Liu, T.; Eastgate, M. D.; Yu, J.-Q. *J. Am. Chem. Soc.* **2016**, *138*, 14554. (e) St John-Campbell, S.; White, A. J. P.; Bull, J. A. *Chem. Sci.* **2017**, *8*, 4840. (f) Liu, Y.; Ge, H. *Nat. Chem.* **2017**, *9*, 26. (g) St John-Campbell, S.; Ou, A. K.; Bull, J. A. *Chem. Eur. J.* **2018**, *24*, 17838. (h) Kapoor, M.; Liu, D.; Young, M. C. *J. Am. Chem. Soc.* **2018**, *140*, 6818.

(17) (a) Davies, H. M. L.; Manning, J. R. *Nature* **2008**, *451*, 417. (b) Doyle, M. P.; Duffy, R.; Ratnikov, M.; Zhou, L. *Chem. Rev.* **2010**, *110*, 704. For recent selected examples, see: (c) He, J.;

Hamann, L. G.; Davies, H. L. M.; Beckwith, R. E. J. *Nat. Commun.* **2015**, *6*, 5943. (d) Bedell, T. A.; Hone, G. A. B.; Valette, D.; Yu, J.-Q.; Davies, H. M. L.; Sorensen, E. J. *Angew. Chem. Int. Ed.* **2016**, *55*, 8270.

(18) (a) Rueping, M.; Vila, C.; Koenigs, R. M.; Poscharny, K.; Fabry, D. C. *Chem. Commun.* **2011**, *47*, 2360. (b) Hari, D. P.; König, B. *Org. Lett.* **2011**, *13*, 3852. (c) Beatty, J. W.; Stephenson, C. R. J. *Acc. Chem. Res.* **2015**, *48*, 1474.

(19) (a) Li, C.-J. *Acc. Chem. Res.* **2009**, *42*, 335. (b) Klussmann, M.; Sureshkumar, D. *Synthesis* **2011**, 353. (c) Girard, S. A.; Knauber, T.; Li, C.-J. *Angew. Chem. Int. Ed.* **2014**, *53*, 74.

(20) For hydrogen atom transfer strategies, see: (a) Yoshikai, N.; Mieczkowski, A.; Matsumoto, A.; Ilies, L.; Nakamura, E. *J. Am. Chem. Soc.* **2010**, *132*, 5568. (b) Capaldo, L.; Ravelli, D. *Eur. J. Org. Chem.* **2017**, *2017*, 2056.

(21) For Ni-catalyzed C–H functionalization of tetrahydrofuran by radical abstraction, see: Liu, D.; Liu, C.; Li, H.; Lei, A. *Angew. Chem. Int. Ed.* **2013**, *52*, 4453.

(22) For photoredox-mediated approaches, see: (a) McNally, A.; Prier, C. K.; MacMillan, D. W. C. *Science* **2011**, *334*, 1114. (b) Noble, A.; MacMillan, D. W. C. *J. Am. Chem. Soc.* **2014**, *136*, 11602. (c) Prier, C. K.; MacMillan, D. W. C. *Chem. Sci.* **2014**, *5*, 4173. (d) Joe, C. L.; Doyle, A. G. *Angew. Chem. Int. Ed.* **2016**, *55*, 4040. (e) Ahneman, D. T.; Doyle, A. G. *Chem. Sci.* **2016**, *7*, 7002. (f) Shaw, M. H.; Shurtleff, V. W.; Terrett, J. A.; Cuthbertson, J. D.; MacMillan, D. W. C. *Science* **2016**, *352*, 1304. (g) Perry, I. B.; Brewer, T. F.; Sarver, P. J.; Schultz, D. M.; DiRocco, D. A.; MacMillan, D. W. C. *Nature* **2018**, *560*, 70. (h) Grainger, R.; Heightman, T. D.; Ley, S. L.; Lima, F.; Johnson, C. N. *Chem. Sci.* **2019**, *10*, 2264.

(23) For Fe-catalyzed C–H oxidation of pyrrolidine ring, see: Osberger, T. J.; Rogness, D. C.; Kohrt, J. T.; Stepan, A. F.; White, M. C. *Nature* **2016**, *537*, 214.

(24) For selected examples proceeding by hydride transfer, see: (a) Jurberg, I. D.; Peng, B.; Wöstefeld, E.; Wasserloos, M.; Maulide, N. *Angew. Chem. Int. Ed.* **2012**, *51*, 1950. (b) Murugesh, V.; Bruneau, C.; Achard, M.; Sahoo, A. R.; Sharma, G. V. M.; Suresh, S. *Chem. Commun.* **2017**, *53*, 10448. (c) Chen, W.; Ma, L.; Paul, A.; Seidel, D. *Nat. Chem.* **2018**, *10*, 165.

(25) (a) Sundararaju, B.; Achard, M.; Sharma, G. V. M.; Bruneau, C. *J. Am. Chem. Soc.* **2011**, *133*, 10340. (b) Millet, A.; Larini, P.; Clot, E.; Baudoin, O. *Chem. Sci.* **2013**, *4*, 2241. (c) Jiang, F.; Achard, M.; Bruneau, C. *Chem. Eur. J.* **2015**, *21*, 14319. (d) Lee, M.; Sanford, M. S. *Org. Lett.* **2017**, *19*, 572. (e) Chen, M.; Liu, F.; Dong, G. *Angew. Chem. Int. Ed.* **2018**, *57*, 3815.

(26) For selected reviews, see: (a) Doye, S. *Angew. Chem. Int. Ed.* **2001**, *40*, 3351. (b) Campos, K. R. *Chem. Soc. Rev.* **2007**, *36*, 1069. (c) Mitchell, E. A.; Peschiulli, A.; Lefevre, N.; Meerpoel, L.; Maes, B. U. W. *Chem. Eur. J.* **2012**, *18*, 10092. (d) Vo, C.-V. T.; Bode, J. W. *J. Org. Chem.* **2014**, *79*, 2809. (e) Seidel, D. *Acc. Chem. Res.* **2015**, *48*, 317. (f) Antermite, D.; Degennaro, L.; Luisi, R. *Org. Biomol. Chem.* **2017**, *15*, 34. (g) Liu, G.-Q.; Opatz, T. *Adv. Heterocycl. Chem.* **2018**, *125*, 107. (h) Gonnard, L.; Guérinot, A.; Cossy, J. *Tetrahedron* **2019**, *75*, 145.

(27) For selected examples see: (a) Beak, P.; Kerrick, S. T.; Wu, S.; Chu, J. *J. Am. Chem. Soc.* **1994**, *116*, 3231. (b) Campos, K. R.; Klapars, A.; Waldman, J. H.; Dormer, P. G.; Chen, C. *J. Am. Chem. Soc.* **2006**, *128*, 3538. (c) Stead, D.; Carbone, G.; O'Brien, P.; Campos, K. R.; Coldham, I.; Sanderson, A. *J. Am. Chem. Soc.* **2010**, *132*, 7260. (d) Beng, T. K.; Gawley, R. E. *J. Am. Chem. Soc.* **2010**, *132*, 12216. (e) Hodgson, D. M.; Kloesges, J. *Angew. Chem. Int. Ed.* **2010**, *49*, 2900. (f) Seel, S.; Thaler, T.; Takatsu, K.; Zhang, C.; Zipse, H.; Straub, B. F.; Mayer, P.; Knochel, P. *J. Am. Chem. Soc.* **2011**, *133*, 4774. (g) Cordier, C. J.; Lundgren, R. J.; Fu, G. C. *J. Am. Chem. Soc.* **2013**, *135*, 10946. (h) Firth, J. D.; O'Brien, P.; Ferris, L. *J. Am. Chem. Soc.* **2016**, *138*, 651.

(28) Ishii, Y.; Chatani, N.; Kakiuchi, F.; Murai, S. *Organometallics* **1997**, *16*, 3615.

(29) Ishii, Y.; Chatani, N.; Kakiuchi, F.; Murai, S. *Tetrahedron Lett.* **1997**, *38*, 7565.

(30) Chatani, N.; Asaumi, T.; Ikeda, T.; Yorimistu, S.; Ishii, Y.; Kakiuchi, F.; Murai, S. *J. Am. Chem. Soc.* **2000**, *122*, 12882.

(31) Pastine, S. J.; Gribkov, D. V.; Sames, D. *J. Am. Chem. Soc.* **2006**, *128*, 14220.

(32) (a) Prokopcová, H.; Bergman, S. D.; Aelvoet, K.; Smout, V.; Herrebout, W.; Van der Veken, B.; Meerpoel, L.; Maes, B. U. W. *Chem. Eur. J.* **2010**, *16*, 13063. (b) Peschiulli, A.; Smout, V.; Storr, T. E.; Mitchell, E. A.; Eliáš, Z.; Herrebout, W.; Berthelot, D.; Meerpoel, L.; Maes, B. U. W. *Chem. Eur. J.* **2013**, *19*, 10378.

(33) Gribkov, D. V.; Pastine, S. J.; Schnürch, M.; Sames, D. *J. Am. Chem. Soc.* **2007**, *129*, 11750.

(34) For a systematic study and alternative conditions for pyridine removal, see: Smout, V.; Peschiulli, A.; Verbeeck, S.; Mitchell, E. A.; Herrebout, W.; Bultinck, P.; Vande Velde, C. M. L.; Berthelot, D.; Meerpoel, L.; Maes, B. U. W. *J. Org. Chem.* **2013**, *78*, 9803.

(35) Schwarz, M. C.; Dastbaravardeh, N.; Kirchner, K.; Schnürch, M.; Mihovilovic, M. D. *Monatsh. Chem.* **2013**, *144*, 539.

(36) Spangler, J. E.; Kobayashi, Y.; Verma, P.; Wang, D.-H.; Yu, J.-Q. *J. Am. Chem. Soc.* **2015**, *137*, 11876.

(37) For a review of Pd^{II}/Pd^{0} C–H functionalization, see: Chen, X.; Engle, K. M.; Wang, D.-H.; Yu, J.-Q. *Angew. Chem. Int. Ed.* **2009**, *48*, 5094.

(38) Jain, P.; Verma, P.; Xia, G.; Yu, J.-Q. *Nat. Chem.* **2017**, *9*, 140.

(39) For a review on BINOL-derived phosphate ligands in asymmetric catalysis, see: Parmar, D.; Sugiono, E.; Raja, S.; Rueping, M. *Chem. Rev.* **2014**, *114*, 9047.

(40) For a single example of complementary C–H arylation of tetrahydroisoquinoline at the benzylic position, see: Dastbaravardeh, N.; Kirchner, K.; Schnürch, M.; Mihovilovic, M. D. *J. Org. Chem.* **2013**, *78*, 658.

(41) Jiang, H.-J.; Zhong, X.-M.; Yu, J.; Zhang, Y.; Zhang, X.; Wu, Y.-D.; Gong, L.-Z. *Angew. Chem. Int. Ed.* **2019**, *58*, 1803.

(42) Greßies, S.; Klauck, F. J. R.; Kim, J. H.; Daniliuc, C. G.; Glorius, F. *Angew. Chem. Int. Ed.* **2018**, *57*, 9950.

(43) For a recent review on TADDOL-based P ligands in C–H activation reaction, see: Pedroni, J.; Cramer, N. *Chem. Commun.* **2015**, *51*, 17647.

(44) Chatani, N.; Asaumi, T.; Yorimistu, S.; Ikeda, T.; Kakiuchi, F.; Murai, S. *J. Am. Chem. Soc.* **2001**, *123*, 10935.

(45) Bergman, S. D.; Storr, T. E.; Prokopková, H.; Aelvoet, K.; Diels, G.; Meerpoel, L.; Maes, B. U. W. *Chem. Eur. J.* **2012**, *18*, 10393.

(46) MacConnell, J. G.; Blum, M. S.; Fales, H. M. *Science* **1970**, *168*, 840.

(47) Kulago, A. A.; Van Steijvoort, B. F.; Mitchell, E. A.; Meerpoel, L.; Maes, B. U. W. *Adv. Synth. Catal.* **2014**, *356*, 1610.

(48) Schinkel, M.; Wang, L.; Bielefeld, K.; Ackermann, L. *Org. Lett.* **2014**, *16*, 1876.

(49) Yi, C. S.; Yun, S. Y. *Organometallics* **2004**, *23*, 5392.

(50) Herzon, S. B.; Hartwig, J. F. *J. Am. Chem. Soc.* **2007**, *129*, 6690.

(51) Eisenberger, P.; Ayinla, R. O.; Lauzon, J. M. P.; Schafer, L. L. *Angew. Chem. Int. Ed.* **2009**, *48*, 8361.

(52) Chong, E.; Brandt, J. W.; Schafer, L. L. *J. Am. Chem. Soc.* **2014**, *136*, 10898.

(53) Payne, P. R.; Garcia, P.; Eisenberger, P.; Yim, J. C.-H.; Schafer, L. L. *Org. Lett.* **2013**, *15*, 2182.

(54) DeBoef, B.; Pastine, S. J.; Sames, D. *J. Am. Chem. Soc.* **2004**, *126*, 6556.
(55) For a related Co-catalyzed transfer hydrogenation of various *N*-[(vinyl)silyl]heterocycles, see: Bolig, A. D.; Brookhart, M. *J. Am. Chem. Soc.* **2007**, *129*, 14544.
(56) Lahm, G.; Opatz, T. *Org. Lett.* **2014**, *16*, 4201.
(57) Tahara, Y.; Michino, M.; Ito, M.; Kanyiva, K. S.; Shibata, T. *Chem. Commun.* **2015**, *51*, 16660.
(58) Tran, A. T.; Yu, J.-Q. *Angew. Chem. Int. Ed.* **2017**, *56*, 10530.
(59) Affron, D. P.; Davis, O. A.; Bull, J. A. *Org. Lett.* **2014**, *16*, 4956.
(60) Nack, W. A.; Wang, B.; Wu, X.; Jiao, R.; He, G.; Chen, G. *Org. Chem. Front.* **2016**, *3*, 561.
(61) Affron, D. P.; Bull, J. A. *Eur. J. Org. Chem.* **2016**, *2016*, 139.
(62) Feng, R.; Wang, B.; Liu, Y.; Liu, Z.; Zhang, Y. *Eur. J. Org. Chem.* **2015**, *2015*, 142.
(63) For the synthesis of a Pd(IV) complex as competent precatalyst see: (a) Vicente J., Arcas A., Juliá-Hernández F., Bautista D.; *Angew. Chem. Int. Ed.* **2011**, *50*, 6896. For a DFT study on the mechanism of a related Pd-catalyzed, AQ-assisted C(sp^3)–H arylation with aryl bromides, see: (b) Wei, Y.; Tang, H.; Cong, X.; Rao, B.; Wu, C.; Zeng, X. *Org. Lett.* **2014**, *16*, 2248.
(64) Yang, X.; Sun, T.-Y.; Rao, Y. *Chem. Eur. J.* **2016**, *22*, 3273.
(65) Berger, M.; Chauhan, R.; Rodrigues, C. A. B.; Maulide, N. *Chem. Eur. J.* **2016**, *22*, 16805.
(66) (a) Yu, Q.-Y.; Zhong, H.-M.; Sun, W.-W.; Zhang, S.-J.; Cao, P.; Dong, X.-P.; Qin, H.-B.; Liu, J.-K.; Wu, B. *Asian J. Org. Chem.* **2016**, *5*, 608. (b) Zhang, S.-J.; Sun, W.-W.; Yu, Q.-Y.; Cao, P.; Dong, X.-P.; Wu, B. *Tetrahedron Lett.* **2017**, *58*, 606.
(67) Hacksell, U.; Arvidsson, L. E.; Svensson, U.; Nilsson, J. L. G.; Sanchez, D.; Wikstroem, H.; Lindberg, P.; Hjorth, S.; Carlsson, A. *J. Med. Chem.* **1981**, *24*, 1475.
(68) Mondal, B.; Roy, B.; Kazmaier, U. *J. Org. Chem.* **2016**, *81*, 11646.
(69) Ye, S.; Yang, W.; Coon, T.; Fanning, D.; Neubert, T.; Stamos, D.; Yu, J.-Q. *Chem. Eur. J.* **2016**, *22*, 4748.
(70) Maetani, M.; Zoller, J.; Melillo, B.; Verho, O.; Kato, N.; Pu, J.; Comer, E.; Schreiber, S. L. *J. Am. Chem. Soc.* **2017**, *139*, 11300.
(71) Kato, N.; Comer, E.; Sakata-Kato, T.; Sharma, A.; Sharma, M.; Maetani, M.; Bastien, J.; Brancucci, N. M.; Bittker, J. A.; Corey, V.; Clarke, D.; Derbyshire, E. R.; Dornan, G. L.; Duffy, S.; Eckley, S.; Itoe, M. A.; Koolen, K. M. J.; Lewis, T. A.; Lui, P. S.; Lukens, A. K.; Lund, E.; March, S.; Meibalan, E.; Meier, B. C.; McPhail, J. A.; Mitasev, B.; Moss, E. L.; Sayes, M.; Van Gessel, Y.; Wawer, M. J.; Yoshinaga, T.; Zeeman, A.-M.; Avery, V. M.; Bhatia, S. N.; Burke, J. E.; Catteruccia, F.; Clardy, J. C.; Clemons, P. A.; Dechering, K. J.; Duvall, J. R.; Foley, M. A.; Gusovsky, F.; Kocken, C. H. M.; Marti, M.; Morningstar, M. L.; Munoz, B.; Neafsey, D. E.; Sharma, A.; Winzeler, E. A.; Wirth, D. F.; Scherer, C. A.; Schreiber, S. L. *Nature* **2016**, *538*, 344.
(72) Verho, O.; Maetani, M.; Melillo, B.; Zoller, J.; Schreiber, S. L. *Org. Lett.* **2017**, *19*, 4424.
(73) Parella, R.; Babu, S. A. *J. Org. Chem.* **2015**, *80*, 2339.
(74) Probst, N. P.; Grelier, G.; Dahaoui, S.; Alami, M.; Gandon, V.; Messaoudi, S. *ACS Catal.* **2018**, *8*, 7781.
(75) Zhang, S.-Y.; Li, Q.; He, G.; Nack, W. A.; Chen, G. *J. Am. Chem. Soc.* **2013**, *135*, 12135.
(76) Yang, Q.; Yang, S.-D. *ACS Catal.* **2017**, *7*, 5220.
(77) Zhu, Q.; Ji, D.; Liang, T.; Wang, X.; Xu, Y. *Org. Lett.* **2015**, *17*, 3798.
(78) Miao, J.; Yang, K.; Kurek, M.; Ge, H. *Org. Lett.* **2015**, *17*, 3738.
(79) (a) Sun, W.-W.; Cao, P.; Mei, R.-Q.; Li, Y.; Ma, Y.-L.; Wu, B. *Org. Lett.* **2014**, *16*, 480. (b) Zhang, S.-J.; Sun, W.-W.; Cao, P.; Dong, X.-P.; Liu, J.-K.; Wu, B. *J. Org. Chem.* **2016**, *81*, 956.
(80) Heinze-Krauss, I.; Angehrn, P.; Charnas, R. L.; Gubernator, K.; Gutknecht, E.-M.; Hubschwerlen, C.; Kania, M.; Oefner, C.; Page, M. G. P.; Sogabe, S.; Specklin, J.-L.; Winkler, F. *J. Med. Chem.* **1998**, *41*, 3961.
(81) Wasa, M.; Chan, K. S. L.; Zhang, X.-G.; He, J.; Miura, M.; Yu, J.-Q. *J. Am. Chem. Soc.* **2012**, *134*, 18570.
(82) He, J.; Wasa, M.; Chan, K. S. L.; Yu, J.-Q. *J. Am. Chem. Soc.* **2013**, *135*, 3387.
(83) Antermite, D.; Affron, D. P.; Bull, J. A. *Org. Lett.* **2018**, *20*, 3948.
(84) Bourin, M.; Chue, P.; Guillon, Y. *CNS Drug Rev.* **2001**, *7*, 25.
(85) Van Steijvoort, B. F.; Kaval, N.; Kulago, A. A.; Maes, B. U. W. *ACS Catal.* **2016**, *6*, 4486.
(86) He, G.; Chen, G. *Angew. Chem. Int. Ed.* **2011**, *50*, 5192.
(87) Achan, J.; Talisuna, A. O.; Erhart, A.; Yeka, A.; Tibenderana, J. K.; Baliraine, F. N.; Rosenthal, P. J.; D'Alessandro, U. *Malar. J.* **2011**, *10*, 144.
(88) O'Donovan, D. H.; Aillard, P.; Berger, M.; de la Torre, A.; Petkova, D.; Knittl-Frank, C.; Geerdink, D.; Kaiser, M.; Maulide, N. *Angew. Chem. Int. Ed.* **2018**, *57*, 10737.
(89) (a) Willcox, D.; Chappell, B. G. N.; Hogg, K. F.; Calleja, J.; Smalley, A. P.; Gaunt, M. J. *Science* **2016**, *354*, 851. (b) Hogg, K. F.; Trowbridge, A.; Alvarez-Pérez, A.; Gaunt, M. J. *Chem. Sci.* **2017**, *8*, 8198. (c) Cabrera-Pardo, J. R.; Trowbridge, A.; Nappi, M.; Ozaki, K.; Gaunt, M. J. *Angew. Chem. Int. Ed.* **2017**, *56*, 11958.
(90) Topczewski, J. J.; Cabrera, P. J.; Saper, N. I.; Sanford, M. S. *Nature* **2016**, *531*, 220.
(91) Beer, B.; Stark, J.; Krieter, P.; Czobor, P.; Beer, G.; Lippa, A.; Skolnick, P. *J. Clin. Pharmacol.* **2004**, *44*, 1360.
(92) Coe, J. W.; Brooks, P. R.; Vetelino, M. G.; Wirtz, M. C.; Arnold, E. P.; Huang, J.; Sands, S. B.; Davis, T. I.; Lebel, L. A.; Fox, C. B.; Shrikhande, A.; Heym, J. H.; Schaeffer, E.; Rollema, H.; Lu, Y.; Mansbach, R. S.; Chambers, L. K.; Rovetti, C. C.; Schulz, D. W.; Tingley, F. D.; O'Neill, B. T. *J. Med. Chem.* **2005**, *48*, 3474.
(93) Walker, N.; Howe, C.; Glover, M.; McRobbie, H.; Barnes, J.; Nosa, V.; Parag, V.; Bassett, B.; Bullen, C. *N. Engl. J. Med.* **2014**, *371*, 2353.
(94) Dewyer, A. L.; Zimmerman, P. M. *ACS Catal.* **2017**, *7*, 5466.
(95) Aguilera, E. Y.; Sanford, M. S. *Organometallics* **2019**, *38*, 138.
(96) Cabrera, P. J.; Lee, M.; Sanford, M. S. *J. Am. Chem. Soc.* **2018**, *140*, 5599.